



POLYTECHNIC UNIVERSITY OF BUCHAREST
ELECTRICAL ENGINEERING DOCTORAL SCHOOL

DOCTORAL THESIS

Doctoral Thesis Summary

Numerical and experimental models of electromagnetic field and heat transfer
in special electric machines

Scientific Adviser

Prof. PhD. Eng. Alexandru – Mihail Morega

Doctoral Student

Eng. Ioana Ionică

This page is intentionally left blank

Summary

DOCTORAL THESIS CHAPTERS STRUCTURE	5
CHAPTER 1 INTRODUCTION	7
1.1. DC limited angle torque motor	7
1.2. DC-LATM Particularities and advantages	7
1.3. DC-LATM Applications	7
CHAPTER 2. MODELING STAGES	7
2.1. Electromagnetic field and heat transfer in DC-LATM motors	7
2.2. Electromagnetic field problem.....	8
2.2.1. Physical model	8
2.2.2. Mathematical model for the electromagnetic field problem in DC-LATM.....	8
2.3. Heat transfer problems in DC-LATM.....	9
2.3.1. Physical-mathematical model	9
CHAPTER 3 MODELING OF DC LIMITED ANGLE TORQUE MOTORS	10
3.1. Introduction	10
3.2. DC-LATM-S design.....	10
3.2.1. The constructive solution 1	10
3.2.2. The constructive solution 2.....	11
3.2.3. The three-dimensional modelling.....	11
3.3. DC limited angle torque motor type DC-LATM-CR.....	12
3.3.1. The two-dimensional modelling.....	12
CHAPTER 4 DC Limited Angle Torque Motors TYPE DC-LATM-CI-C	13
4.1. The two-dimensional model of the DC-LATM-CI-C	13
4.1.1. Iron-Silicon variant for the stator stack (DC-LATM-CI-B).....	14
4.1.1.1. The influence of rotor construction solutions on torque-angle curve for DC-LATM-CI-B	14
4.1.2. Iron-Cobalt variant for the stator stack (DC-LATM-CI-C)	15
4.1.2.1. The analysis of rotor construction solutions for torque-angle curve - DC-LATM-CI-C	16
4.1.2.2. OI Spacers – The deviation torque angle curves from the ideal curve.....	17
4.1.2.3. OI spacers - Deviation of the torque-angle curve from the symmetric curve.....	18
4.1.2.4. Al spacers - Deviation of the torque-angle curve from the ideal curve	19
4.1.2.5. Al spacers - Deviation of the torque-angle curve from the symmetric curve.....	19
4.1.2.6. Study on the numerical analysis of the two-dimensional model for the DC-LATM-CI-C motor	19
4.2. The three-dimensional model	20

4.2.1. Using finite elements of “infinite” type.....	20
CHAPTER 5 THERMAL MODELING OF A DC LIMITED ANGLE TORQUE MOTOR, DC-LATM-CI-C TYPE	22
5.1. Introduction	22
5.2. DC-LATM-CI-C mounted in a non-magnetic stainless-steel device – Variant 1.....	22
5.3. DC-LATM-CI-C mounted in a non-magnetic stainless-steel device – Variant 2.....	23
5.4. DC-LATM-CI-C mounted in case	23
5.4.1. DC-LATM current: $I = 1.33$ A.....	23
5.4.2. DC-LATM current: $I = 1$ A	24
5.5. The experimental results of DC-LATM-CI-C thermal test. Comparison of numerical results with experimental results	25
5.5.1. DC-LATM current: $I = 1$ A	25
5.5.2. DC-LATM current: $I = 1.33$ A.....	25
CHAPTER 6. STUDY ON THE DC-LATM APPROACH IN VARIOUS FIELD APPLICATIONS - MATERIALS AND TECHNOLOGICAL FLOW	25
6.1. Specifications or standards	26
6.2. Selection of non-suitable materials for space applications.....	26
6.2.1. Purchase of materials.....	26
CHAPTER 7. dc LIMITED ANGLE TORQUE MOTOR – EXPERIMENTALS MODELS	26
CONCLUSIONS.....	28
C.1. General conclusions	28
C.2. Original contributions	28
C.3. Development perspectives.....	29
ANNEX A1 – GENERAL FORM FOR THE MAGNETIC FIELD.....	29
ANNEX A2. TRL LEVELS	30
ANNEX A3. ESA STANDARDS - SELECTION.....	30
ANNEX A4. MATERIALS LIST SPACEMATDB - Space Materials DataBase.....	30
ANNEX A5. MATERIALS USED IN SPACE APPLICATIONS AND THE RELEVANCE OF SPACE PARAMETERS ON MATERIAL SELECTION.....	30
ANNEX A6. MATERIALS LIST - DML.....	30
ANNEX A7. PROCESSES LIST - DPL.....	30
ANNEX A8. THE STAGES OF THE TECHNOLOGICAL PROCESS OF A DC-LATM.....	30
Bibliography	31

Keywords: DC limited angle torque motor, special electric machines, physical model, mathematical model, numerical analysis, two-dimensional model, three-dimensional model, finite element method, optimal design, electromagnetic field, heat transfer, linear regression, relative deviation, absolute deviation, space, vacuum, ROSA, ESA, EM, QM, experimental model, DC-LATM.

DOCTORAL THESIS CHAPTERS STRUCTURE

The doctoral thesis “Numerical and experimental models of electromagnetic field and heat transfer in special electric machines” is structured in 7 chapters, conclusions, annexes and bibliography.

Chapter 1, “INTRODUCTION”, presents introductory notions about DC Limited Angle Torque Motors - DC-LATM and consists of three subchapters. 1.1. “DC Limited Angle Torque Motors” is the first subchapter and presents the situation and types of DC-LATM manufactured nationally and worldwide. The second subchapter, 1.2. “Particularities and advantages of DC-LATM” presents the structure, advantages, particularities and technical characteristics of DC-LATM. In the last subchapter, 1.3. “DC-LATM applications”, the applications of these types of motors are highlighted.

Chapter 2, “MODELING STAGES”, deals with the approach in analyzing a problem. The first subchapter, 2.1 “Electromagnetic field and heat transfer in DC-LATM motors” presents the steps for solving electromagnetic field problems and heat transfer. Subchapters 2.2 "Electromagnetic field problem" and 2.3 "DC-LATM heat transfer problems" cover the electromagnetic field and heat transfer problems. In sections 2.2.1, 2.2.2 and 2.3.1, are established the simplifying physical assumptions of the analysis and the operating regime. The main physical quantities that characterize the operation of DC-LATM are identified. The dependency relationships between the quantities determined by the physical model and the expression in a mathematical form are presented. The dependency relations between the quantities determined in the physical model and the expression in a consistent mathematical form are presented (existence and uniqueness of the solution) Information can be found in ANNEX A1.

Chapter 3, “Modeling of DC Limited Angle Torque Motors,” is dedicated to the numerical models for DC-LATM. First subchapter 3.1. “Introduction” shows the calculation of specific DC-LATM sizes and characteristics using a software package. Subchapter 3.2. “DC-LATM-S design” describes the numerical modeling and the results for a DC-LATM considering two constructive solutions. Subchapter 3.3. “DC Limited Angle Torque Motors type DC-LATM-CR” shows the numerical modeling and the results obtained for this type of motor. The description and formulation of the problem, the presentation of the particularities of each motor, the results of the numerical study and their interpretation are realized for each of the two DC-LATM models.

Chapter 4, “DC Limited Angle Torque Motor type DC-LATM-CI-C”, describes the numerical models for a particular case of DC-LATM, chosen for the special constructive characteristics that it presents. Subchapter, 4.1. “Two-dimensional model of DC-LATM-CI-C”, presents the particularities, numerical analysis and modeling results obtained for DC-LATM-CI-B and DC-

LATM-CI-C. The numerical analysis of the rotor constructive solutions influence on the torque-angle curve for DC-LATM-CI-B and DC-LATM-CI-C is presented. Different variants of the rotor were analyzed by resizing the auxiliary magnets and the deviation of the torque-angle curve from the ideal characteristic and from the symmetry was calculated. The results obtained are presented and analyzed. In the second subchapter, 4.2. The "three-dimensional model" are numerically analyzed 3D models that eliminate certain simplifying hypotheses of the 2D model and that use finite elements of the "infinite" type.

Chapter 5 "Thermal modeling of a DC Limited Angle Torque Motors type DC-LATM-CI-C" aims to evaluate the thermal behavior of the motor analyzed at Chapter 4. In the subchapters: 5.1. "Introduction", 5.2. "DC-LATM-CI-C mounted in a non-magnetic stainless-steel device - Variant 1", 5.3. "DC-LATM-CI-C mounted in a non-magnetic stainless-steel device - Variant 2", 5.4. "DC-LATM-CI-C mounted in the housing", 5.5. "Experimental thermal test results "DC-LATM-CI-C. Comparison of numerical results with experimental results", different mounting devices of this type of motor are numerically studied. The first two variants consider the motor mounted in devices made of non-magnetic stainless steel. Another option considers the motor mounted in the housing, without being mounted in the system. The thermal study validated by the experiment allows to establish the time in which the temperature in the windings reaches the maximum allowed value.

In Chapter 6 is studied a DC-LATM for military and aerospace applications in materials and technology flow. This information is the input for the analysis of this motor type for space applications. The study is completed by the technological process stages for DC-LATM-CI-D and DC-LATM-CI. ANNEXES A2 ÷ A8 provides supplementary information.

Chapter 7 presents experimental models for two DC-LATMs, subjected to a set of specific DC-LATM measurements and tests (obtaining the torque-angle curve on the operating range). The experimental data obtained from the measurements for DC-LATM-CI-C are compared with the numerical results for the validation of the numerical models.

The last chapter highlights the general conclusions of scientific research and the results obtained in this thesis in the field of DC-LATM motors, personal contributions to this paper and prospects for further development.

CHAPTER 1 INTRODUCTION

This chapter presents the DC limited angle torque motor, with particularities, advantages and applications.

1.1. DC limited angle torque motor

DC motors are used due to the advantages offered by the naturally linear and sufficiently rigid mechanical characteristic. They are designed to operate in the “direct-drive” construction (they are mounted directly on the drive shaft): the rotor yoke on which the magnets are placed acts as the axis of the motor.

This type of motor is predominantly used for precise motion control and is developed for applications where rotation on a certain angular range is the main requirement. These motors have certain advantages: low inertia, they run at higher speeds, dissipate heat better and are more reliable. The major disadvantage is the high cost of the control systems, but this is avoided by using a type of brushless DC motor, called DC-LATM. It belongs to the category of special electric motors and differs from classic electric cars by construction, particularities and applications in which they are used.

The DC-LATM research is based on the analysis of the current situation of these types of motors [1].

The current market for these types of motors has been studied, considering, among other things, the characteristics highlighted by [2-5].

1.2. DC-LATM Particularities and advantages

Mounted in a drive system, DC-LATM is an electromechanical actuator with limited angle. With a simple structure consisting of two subassemblies, stator and rotor, DC-LATM has high reliability.

The advantages of this type of motor are very low cogging torque, high angular acceleration, high power density, high efficiency etc.

1.3. DC-LATM Applications

This type of motor is used for various applications where the volume and weight of the system is a priority (control systems, aerospace applications, any system that requires limited range of rotation, military equipment etc.).

CHAPTER 2. MODELLING STAGES

2.1. Electromagnetic field and heat transfer in DC-LATM motors

The stages of solving the problems of electromagnetic field and heat transfer are the physical model, the associated mathematical model and its solution (by analytical, numerical or hybrid methods).

Numerical modeling is used in the study, establishing the constructive solution and designing

three variants of DC-LATM motor. The first motor, DC-LATM-S, has the specific technical characteristics of TQR-10 / 2-0.35 [4]; DC-LATM-CR has high torque and the specific technical characteristics of TQR-18-1.06-2CH; and the third motor, DC-LATM-CI, is equipped with magnetic field hardening magnets and has specific technical characteristics of TQR-16 / 2-0.35 and TQR-16 / 2-0.35-C. Their main parameter is the maximum torque on a given angular domain, implicitly the torque-angle curve. Numerical analysis offers various advantages, including the reduction of the number of tests (prototypes) as well as manufacturing costs.

2.2. Electromagnetic field problem

The physical model represents the stage in which the laws are identified (which describe the operating principle of DC-LATM) together with the related physical quantities.

2.2.1. Physical model

In this subchapter is formulated, (2.1a), and solved the problem of electromagnetic field in *stationary magnetic regime* for DC-LATM. The sources of the magnetic field are the stator windings and the permanent excitation magnets.

General theorems of the electromagnetic field

This section presents the general theorems of electromagnetic pulse and electromagnetic energy.

Interactions in the electromagnetic field

The thermal equilibrium of a system with its exterior is expressed by the Zeroth Law of Thermodynamics (Maxwell).

2.2.2. Mathematical model for the electromagnetic field problem in DC-LATM

In *stationary magnetic regime* (immobile bodies, constant quantities in time) the laws of the magnetic field are:

$$\begin{cases} \operatorname{div}\mathbf{B} = 0 \Rightarrow \mathbf{B} = \operatorname{rot}\mathbf{A}, - \text{the magnetic flux law} \\ \mathbf{B} = \bar{\mu}\mathbf{H} + \mu_0\mathbf{M}_p \Rightarrow \mathbf{H} = \bar{\mu}^{-1}(\mathbf{B} - \mu_0\mathbf{M}_p) - \sigma \underset{=0}{(\mathbf{v} \times \mathbf{B})} - \text{the material law} \\ \operatorname{rot}\mathbf{H} = \mathbf{J} \Rightarrow \operatorname{rot}(\bar{\mu}^{-1}\operatorname{rot}\mathbf{A}) - \sigma \underset{=0}{(\mathbf{v} \times \mathbf{B})} = \mathbf{J} + \operatorname{rot}(\bar{\mu}^{-1}\mu_0\mathbf{M}_p) - \text{the magnetic circuit law} \end{cases} \quad (2.1)$$

Using the magnetic vector potential, \mathbf{A} , the magnetic circuit law becomes

$$\operatorname{rot} \frac{\operatorname{rot}\mathbf{A}}{\mu} = \mathbf{J} + \operatorname{rot} \frac{\mu_0\mathbf{M}_p}{\mu}. \quad (2.1a)$$

In the numerical analysis of DC-LATM is of interest the magnetic flux density, \mathbf{B} , in the magnetic circuit of the motor and the torque curve as a function of angle, on the operating range of the DC-LATM (Chapters 3 and 4).

The electromagnetic torque, \mathbf{M}_0 [Nm] is the main parameter of DC-LATM and is calculated using Maxwell stress tensor [11, 12]

$$\mathbf{n}_1 \mathbf{T}_2 = -\frac{1}{2} \mathbf{n}_1 (\mathbf{H} \cdot \mathbf{B}) + (\mathbf{n}_1 \cdot \mathbf{H}) \mathbf{B}^T, \quad (2.2)$$

respectively

$$\mathbf{M}_0 = \oint_{\Sigma} (\mathbf{r} - \mathbf{r}_0) \times (\mathbf{n}_1 \cdot \mathbf{T}_2) dS, \quad (2.3)$$

where \mathbf{r}_0 is the radius relative to the axis of rotation and Σ is the frontier.

2.3. Heat transfer problems in DC-LATM

The physical model represents the stage in which the laws are identified (which describe the heat transfer in the studied DC-LATM motors) together with the characteristic physical quantities.

2.3.1. Physical-mathematical model

Heat transfer is made through three mechanisms: thermal conduction (material media), thermal convection (fluid media) and thermal radiation between the surfaces of bodies.

Conduction heat transfer

Thermal conduction equation is (Fourier`s law)

$$\mathbf{q}''_{cond} \stackrel{\text{def}}{=} -k\nabla T, \quad (2.4)$$

where \mathbf{q}''_{cond} [W/m²] is the conduction heat flux, k [W/mK] is the thermal conductivity of the substance, ∇T [K/m] is the temperature gradient. The heat transfer by thermal conduction is performed from higher temperature to lower temperature ($T_1 > T_2$).

Convection heat transfer

The heat transfer between a solid body and a fluid is given by (Newton`s law)

$$q''_{conv} \stackrel{\text{def}}{=} h(T_w - T_{\infty}), \quad (2.12)$$

where T_w is the surface temperature, T_{∞} is the free stream temperature, q''_{conv} [W/m²] is the convection heat flux and h [W/m² K] is the convection heat transfer coefficient.

Radiation heat transfer

gives the maximum heat flux at which the thermal radiation may be emitted by the surface of a body, called an ideal radiator or blackbody (Stefan – Boltzmann`s law) [11]

$$q''_{SB} = \sigma T_S^4, \quad (2.13)$$

where T_S is the absolute temperature of the body surface and σ is Stefan-Boltzmann constant, a universal constant ($\sigma = 5.67 \times 10^{-8}$ W/m²K⁴).

The radiative heat flux emitted by a real surface, called a gray surface, is only a fraction of that emitted by the blackbody (an idealized concept)

$$q''_{SB,b} = \varepsilon \sigma T_S^4, \quad (2.14)$$

where ε is the emissivity.

Interface and limit conditions

Heat transfer in DC-LATM is produced by thermal conduction, thermal convection and thermal radiation. Mathematical models for estimating the temperatures in DC-LATM windings (internal heat source) are developed and analyzed. Transient and stationary regimes

are considered.

For DC-LATM are considered 2D and 3D models, $T_{amb} = 22^\circ \text{C}$ and cooling through natural convection

$$-\mathbf{n} \cdot (-k\nabla T) = h(T_{ext} - T), \quad (2.43)$$

or by radiation toward the environment

$$-\mathbf{n} \cdot (-k\nabla T) = h(T_{inf} - T) + \varepsilon(G - \sigma T^4), \quad (2.44)$$

$$(1 - \varepsilon)G = J_0 - \varepsilon\sigma T^4, \quad (2.45)$$

where T_{inf} is the reference temperature, ε is the surface emissivity, T_{amb} is the ambient temperature, J_0 [Wm^{-2}] is the surface radiosity, G [W/m^2] is the ambient environment irradiation.

The information that were presented in this chapter are used in Chapters 3, 4 and 5 in the numerical analysis of electromagnetic field and heat transfer problems for the DC-LATM.

CHAPTER 3 MODELING OF DC LIMITED ANGLE TORQUE MOTORS

3.1. Introduction

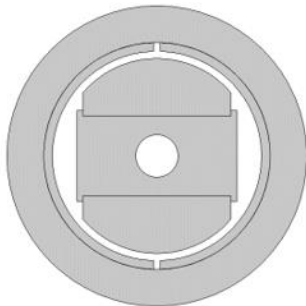
In this chapter numerical models for DC-LATM were integrated using the Finite Element Method [25].

3.2. DC-LATM-S design

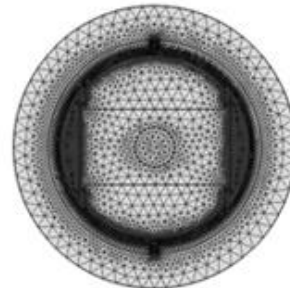
This type of motor is under construction "direct - drive". Two functional variants were analyzed.

3.2.1. The constructive solution 1

The DC-LATM-S constructive solution is shown in Fig. 3.1 a. In the magnetic circuit, soft and hard magnetic materials for rotor and soft magnetic materials for stator are used [4]. The magnetic field problem is solved for the steady state. A FEM mesh was generated considering the motor geometry, Fig. 3.2 a.



a) Computational domain.



b) The FEM mesh.

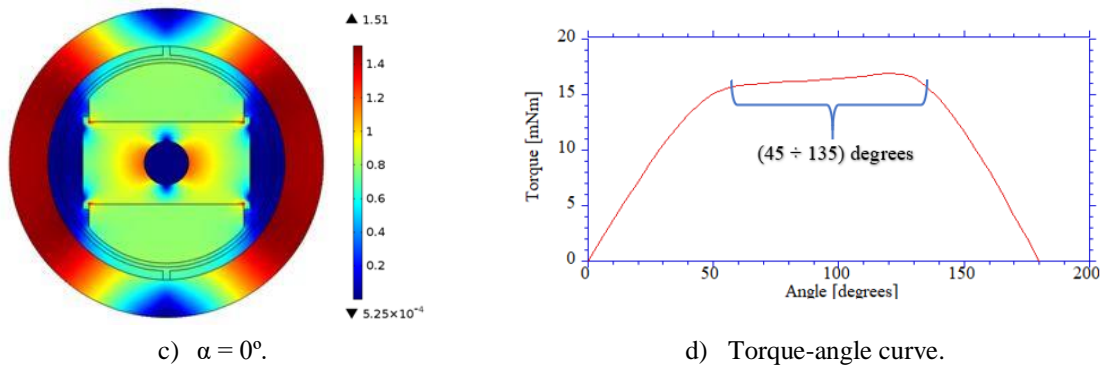


Fig. 3.1. a) Computational domain for DC-LATM-S, Variant 1; b) The FEM mesh; c) \mathbf{B} [T] for $\alpha = 0^\circ$; d) Torque-angle curve.

Figure 3.1, c shows the magnetic flux density. The torque-angle curve is shown in Fig. 3.1 d.

3.2.2. The constructive solution 2

The second constructive solution was made, DC-LATM-S - A (Fig. 3.2, a). In the magnetic circuit, the same magnetic materials are used [4]. The FEM mesh is shown in Fig. 3.2, b.

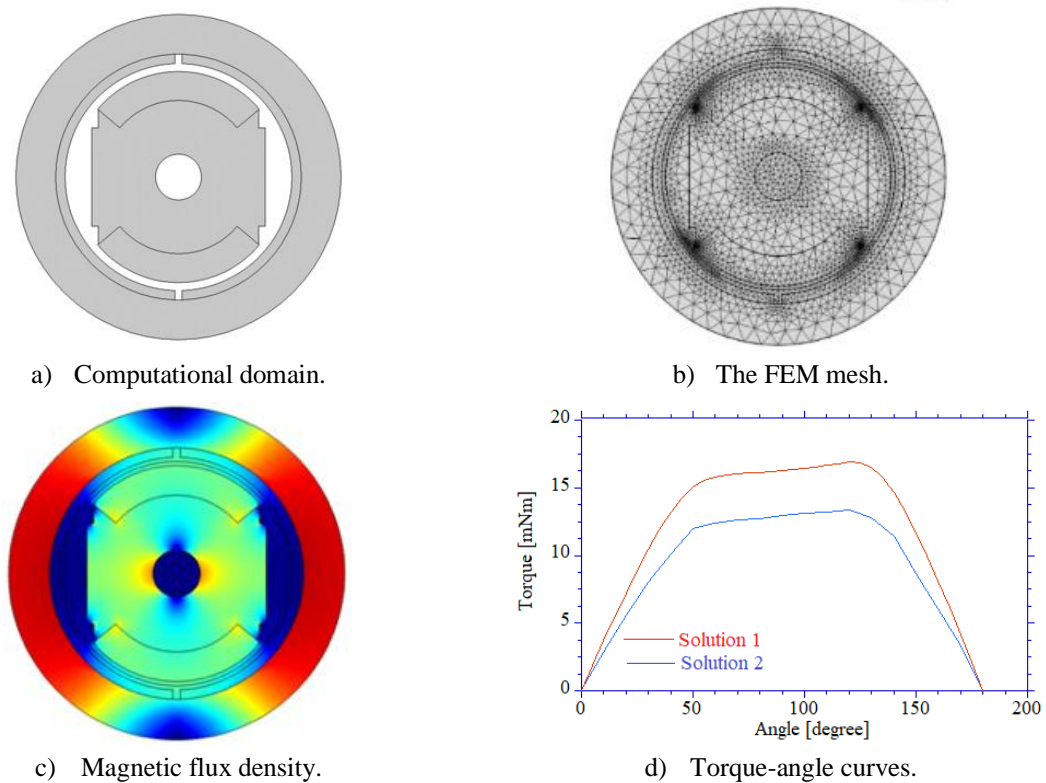


Fig. 3.2. a) Computational domain; b) The FEM mesh; c) \mathbf{B} , max. 1.57 T, min. 0 T; d) Torque-angle curves comparison.

Figures 3.2, c and d show the magnetic flux density and the torque-angle curves, respectively.

3.2.3. The three-dimensional modelling

A three-dimensional numerical analysis of the first variant of DC-LATM-S was performed.

Figure 3.3 shows the constructive parts of the model used in the numerical analysis: (1) the stator stack; (2) stator winding; (3) air gap, (4) magnet, (5) rotor shaft and (6) air domain. The

materials presented in the numerical analysis of the 2D model are used also for the three-dimensional model. The FEM mesh is generated, Fig. 3.3, b.

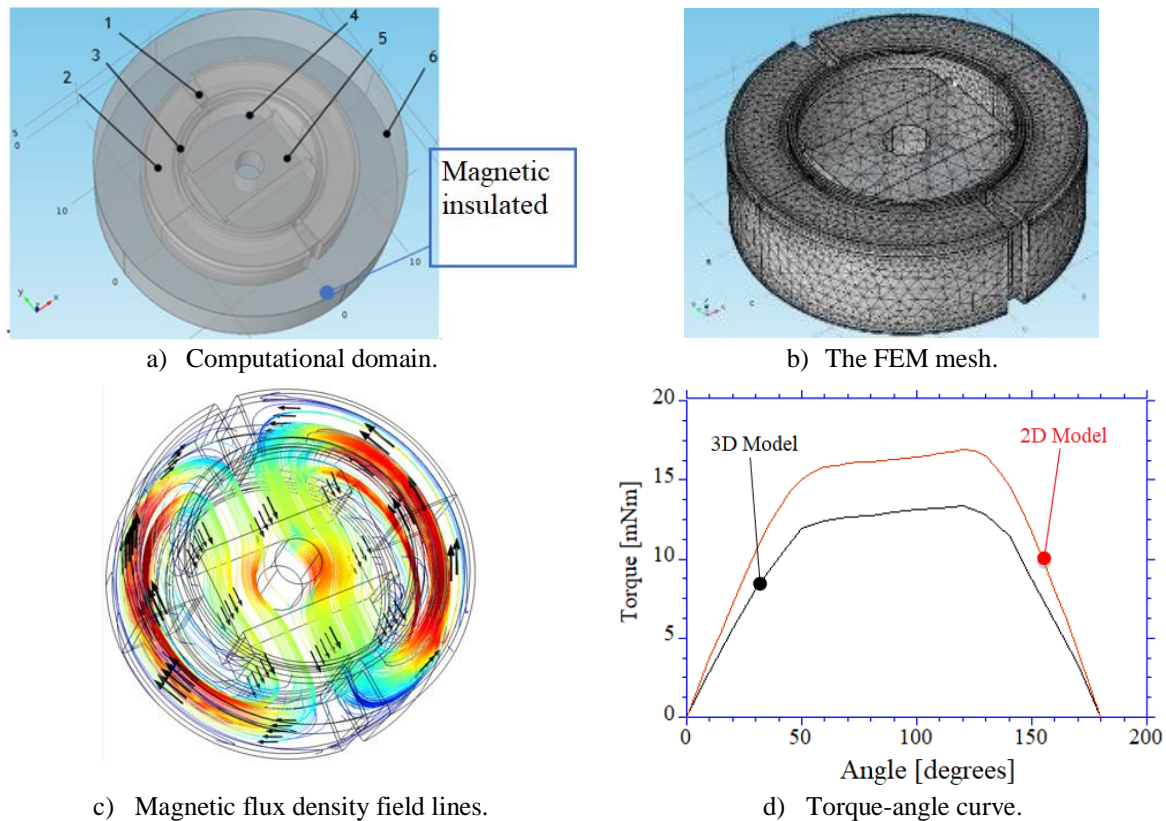


Fig. 3.3. a) DC-LATM-S Computational domain; b) The FEM mesh; c) The spectrum of magnetic field lines, max.1.37 T, min. 0 T; d) Torque-angle curves obtained from 2D and 3D models.

Figures 3.3, c and d show the spectrum of magnetic field lines, respectively the torque-angle curve for 2D and 3D models. The maximum deviation value of the torque obtained in the 2D model compared to the 3D one is 21.03%.

3.3. DC limited angle torque motor type DC-LATM-CR

In this subchapter, DC-LATM-CR is analyzed, a motor which is dual-channel and provides the role of two DC-LATM [4].

3.3.1. The two-dimensional modelling

Analyzing various cases of the constructive solution for this type of motor, results the solution given in Fig. 3.4, a.

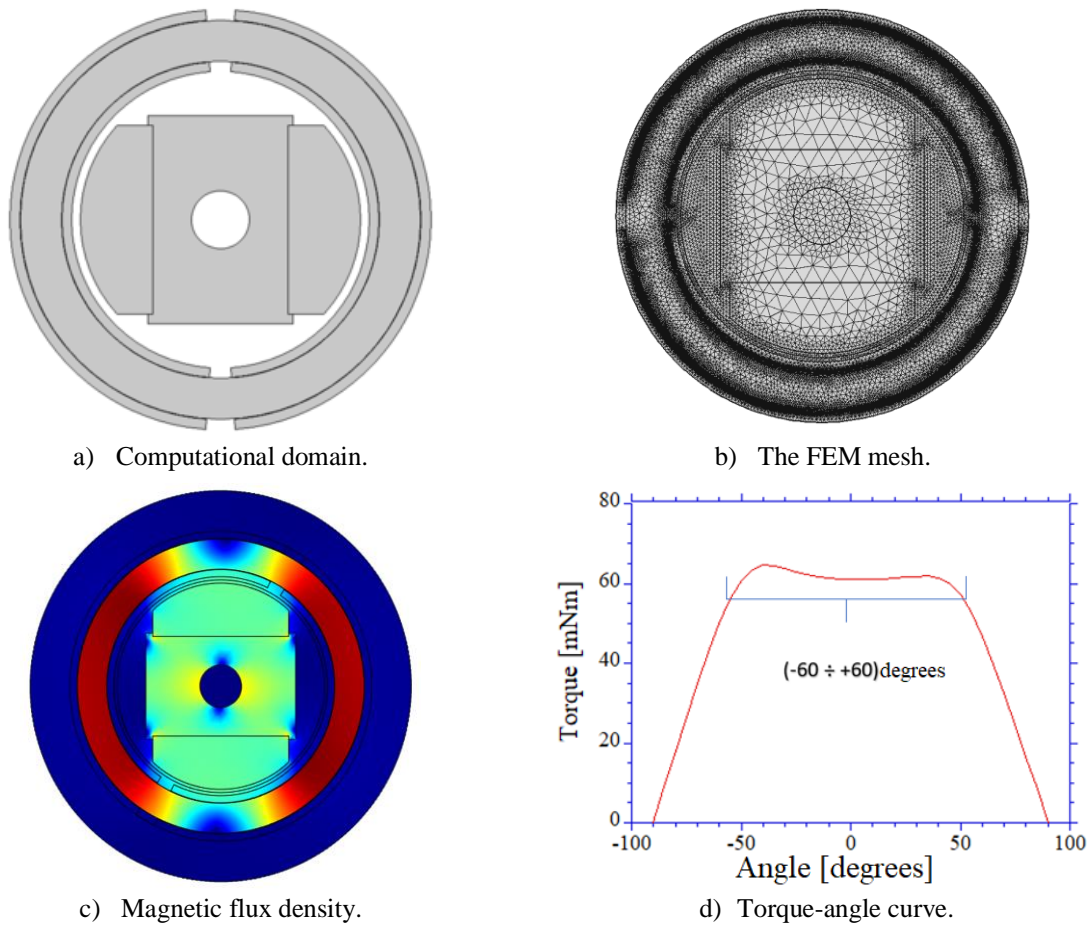


Fig. 3.4. a) Computational domain for DC-LATM-CR; b) The FEM mesh; c) B , max. 2.01 T, min. 0 T. d) Torque-angle curve.

In the construction of the magnetic circuit, soft and hard magnetic materials for rotor and soft magnetic materials for stator are used [4]. The magnetic field problem is solved for the steady state. A FEM mesh was generated considering the geometry of the motor, Fig. 3.4 a).

Figure 3.4, c shows the color map of the magnetic flux density. For the torque-angle curve shown in Figs. 3.4, d a parametric study was performed relative to the stator-rotor position angle.

CHAPTER 4 DC LIMITED ANGLE TORQUE MOTORS TYPE DC-LATM-CI-C

This chapter presents the numerical analysis for DC-LATM-CI-C. This motor has special constructive characteristics - auxiliary magnets in the interpolar axis.

In a first step, 2D approximations will be used for numerical analysis.

4.1. The two-dimensional model of the DC-LATM-CI-C

As a first step of the numerical study, the computational domain is established.

4.1.1. Iron-Silicon variant for the stator stack (DC-LATM-CI-B)

In the construction of the magnetic circuit, soft and hard magnetic materials for rotor and soft magnetic materials for stator are used [4]. The magnetic field problem is solved for the steady state. A FEM mesh was generated considering the geometry of the motor, Fig. 4.1 a.

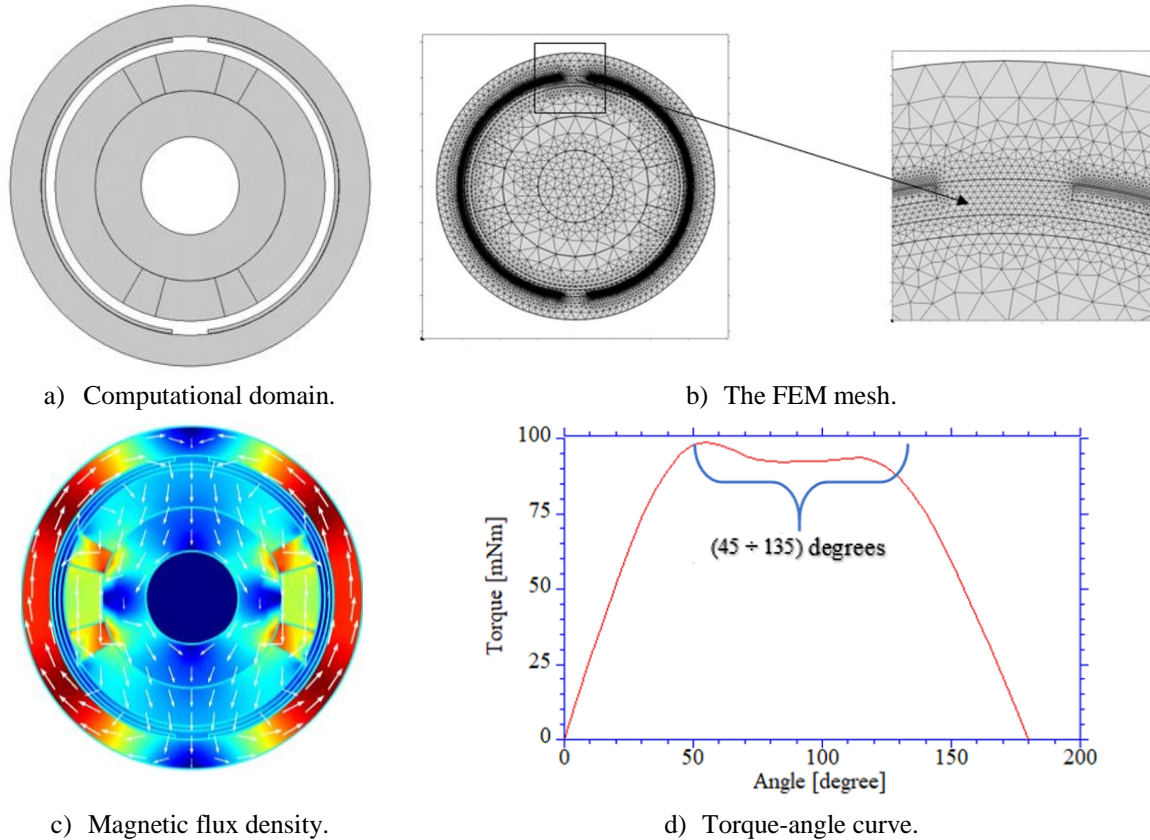


Fig. 4.1. a) Computational domain for DC-LATM-S; b) The FEM mesh; c) Magnetic flux density, max, 2.04 T, min. 0 T; d) Torque-angle curve.

Figures 4.1, c and d show the magnetic flux density, respectively the torque-angle curve.

The results obtained are strongly affected by the simplifying hypotheses. In this case it is a parallel plane problem (end effects are neglected).

4.1.1.1. The influence of rotor construction solutions on torque-angle curve for DC-LATM-CI-B

Starting from the constructive solution 1, different constructive solutions of the rotor were analyzed by resizing the auxiliary magnets, Fig. 4.2.

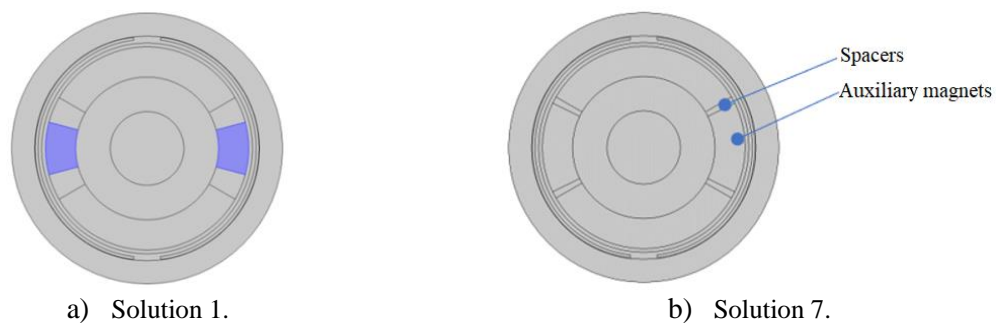


Fig. 4.2. Rotor constructive solutions.

In this numerical study, OI and AI spacers were used.

Figures 4.3, a and b show the magnetic flux density obtained for the OI and AI spacers and Figs. 4.3, c and d show the torque-angle curves calculated for the two variants.

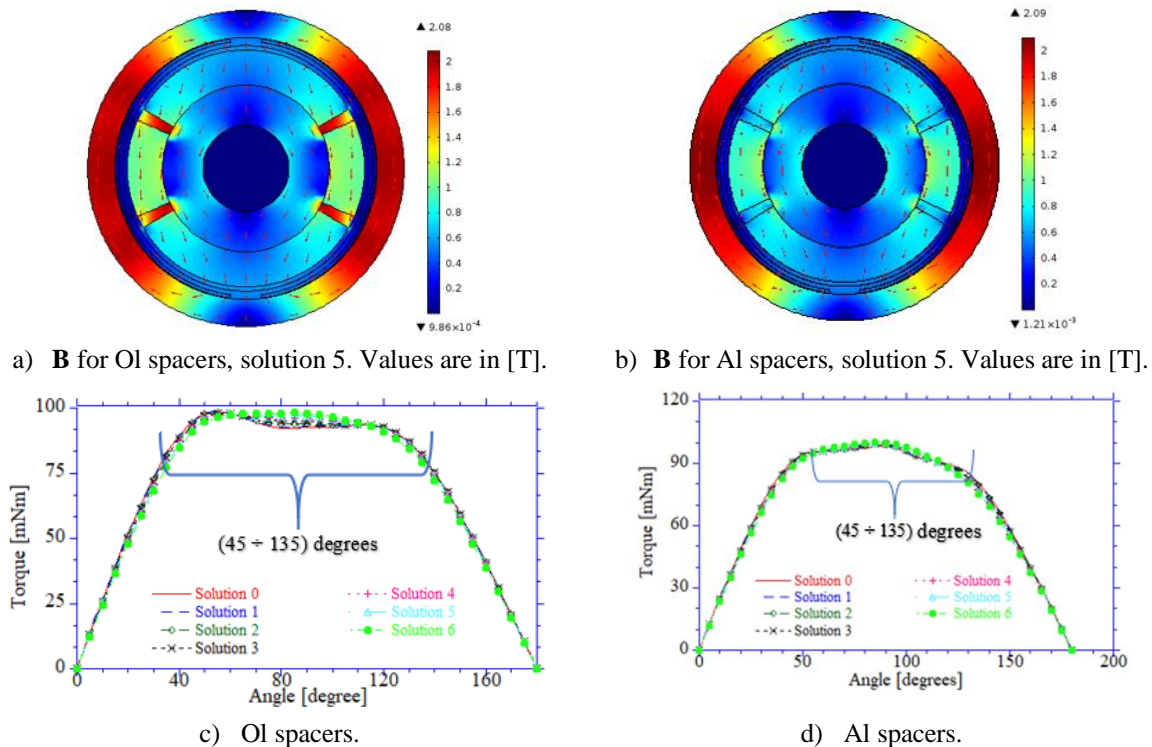


Fig. 4.3. a) and b) The electromagnetic solution obtained for simulating the OI and AI spacers; c) and d) The torque-angle curves for the constructive variants with OI and AI spacers.

A study of the curves of electromagnetic torque as a function of angle on the angular domain (0 ÷ 180 degrees) was performed. Following the analysis, it is observed that solution 5 has a torque-angle curve very close to linearity. Also, the torque obtained for solution 5 is higher compared to solution 0.

It is concluded that the option to avoid is that in which AI is used for spacers. Although the torque is higher, no uniformity of the torque-angle curve is obtained.

4.1.2. Iron-Cobalt variant for the stator stack (DC-LATM-CI-C)

Following the results of the DC-LATM-CI-B study, it was observed that portions of the stator were saturated. Thus, Iron – Cobalt (Fe-Co) will be used for the sheet metal package - DC-LATM-CI-C.

The computational domain and the FEM mesh for DC-LATM-CI-C used in the numerical study are presented in Fig. 4.1, a and b.

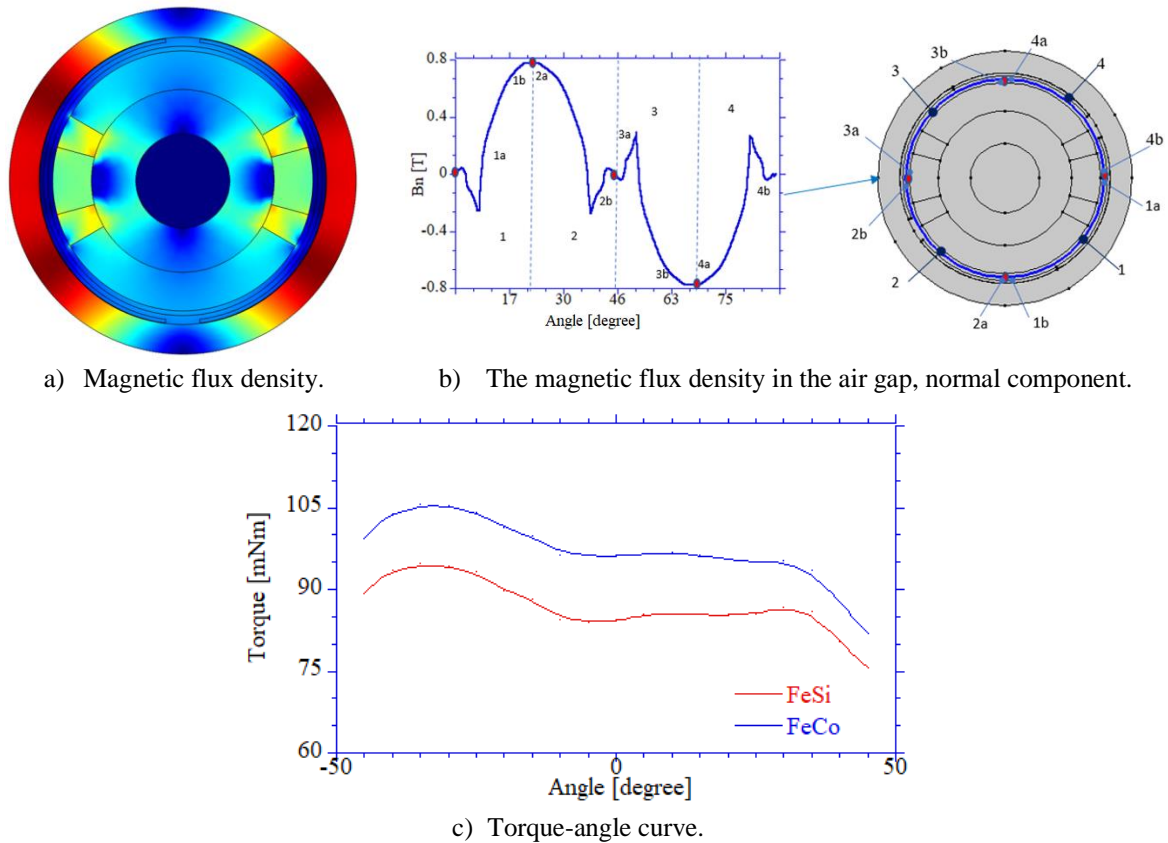


Fig. 4.4. a) Magnetic flux density; b) The air gap distribution of the normal component of magnetic flux density; c) Torque-angle curves for the two models.

Figure 4.4 a shows the magnetic flux density, maximum value 2.31 T. In Fig. 4.4, b is highlighted the magnetic flux density in the air gap, normal component, maximum value 0.79 T. Fig. 4.4, c shows the torque-angle curves of DC-LATM with the stator yoke constructed of FeSi and FeCo, solution 1. The torque error obtained in the models with FeSi (97 mN m) and FeCo (107.87 mN m) for the stator stack was calculated. The difference between the torque values is 10.07%.

4.1.2.1. The analysis of rotor construction solutions for torque-angle curve - DC-LATM-CI-C

Different constructive solutions of the rotor were analyzed by resizing the spacers and implicitly the auxiliary magnets, Fig. 4.2.

In this numerical study, Ol and Al spacers were used.

Figures 4.5, a and b show the magnetic flux density simulated for Ol and Al spacers. Fig. 4.5, c and d highlight the torque-angle curves calculated for the two variants.

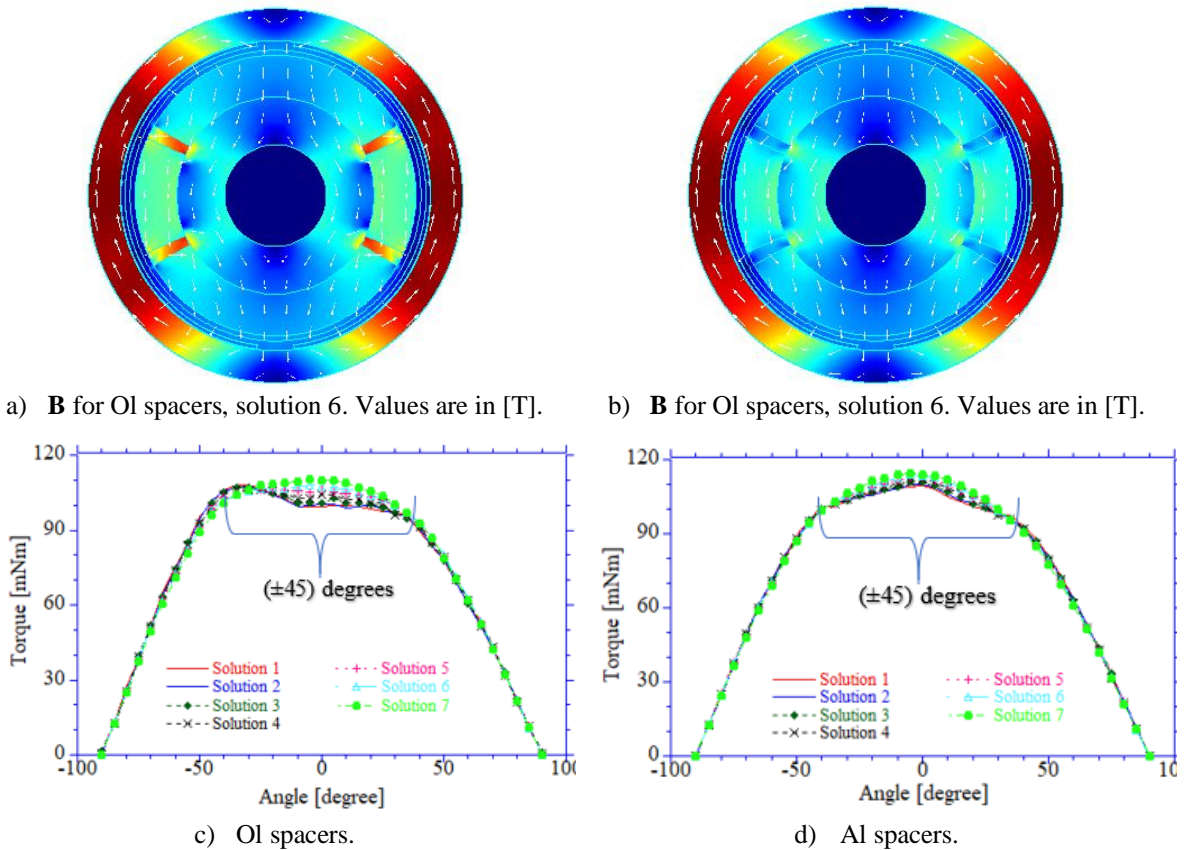


Fig. 4.5. a) and b) The electromagnetic solution obtained for simulating the OI and AI spacers; c) and d) Torque-angle curves for the constructive variants with the OI and AI spacers.

It is observed that solution 6 has a torque-angle curve very close to linearity. The torque obtained for solution 6 has a higher value compared to solution 1. Comparing, it is concluded that is to be avoided the variant in which AI spacers are used.

Next, is presented the study of the torque-angle curves uniformity for the constructive solutions detailed in sections 4.1.1.1 and 4.1.2.1. The deviation of the torque-angle curve from the ideal and symmetric ones was calculated. In the following subchapters, 4.1.2.2 ÷ 4.1.2.5 this analysis is presented.

4.1.2.2. OI Spacers – The deviation torque angle curves from the ideal curve

This section presents the comparative analysis of the torque-angle curve in relation to the ideal curve by determining the simple linear regression.

The equation of the linear trend line for the torque obtained by modeling the variants uses the least squares method so that

$$M = a + bu, \quad (4.1)$$

where M represents the torque of the constructive solution, a represents the point where the trend line intersects the y axis, b represents the slope of the trend line and u represents the angular position.

For the global evaluation of the simple linear regression model, the correlation coefficient, R , is determined using the equation

$$R = \frac{n \left(\sum_{i=1}^{19} u_i M_i \right) - \left(\sum_{i=1}^{19} u_i \right) \left(\sum_{i=1}^{19} M_i \right)}{\sqrt{\left[n \sum_{i=1}^{19} u_i^2 - \left(\sum_{i=1}^{19} u_i \right)^2 \right] \left[n \sum_{i=1}^{19} M_i^2 - \left(\sum_{i=1}^{19} M_i \right)^2 \right]}}, \quad (4.2)$$

in which $n = 19$ and represents the number of values for the torque and the angular position for which the trend line is calculated.

Next, the rate with which the independent variable (angular position) significantly influences the variation of the dependent variable (torque) is expressed. This assessment is based on the analysis of the coefficient of determination R^2 .

In this study, the absolute deviation from the ideal curve, d , is defined by

$$d = M_{ideal} - M_{real}. \quad (4.3)$$

In this study, the relative deviation from the ideal curve, d_r , is defined by

$$d_r = \frac{M_{real} - M_{ideal}}{M_{ideal}} \cdot 100, \quad (4.4)$$

where M_{ideal} is the torque corresponding to the ideal curve and M_{real} is the torque relative to the actual curve.

This evaluation selects the constructive solutions 5 and 6 of the motor. For each constructive solution, simple linear regression was analyzed. The results are presented, including deviations d and d_r from the ideal curve. These are larger for variant 6 compared to variant 5. The absolute deviation-angle curve is also presented. In both cases (constructive solutions 5 and 6), the maximum deviation is 45° . For the other constructive solutions, the deviations show the distance of the torques from linearity.

4.1.2.3. OI spacers - Deviation of the torque-angle curve from the symmetric curve

The symmetric curve was calculated by averaging the torque values corresponding to the symmetrical angles, $-\alpha$ and α . In this study, the absolute deviations d_s and relative d_{rs} , are given by

$$d_s = M_{real} - M_{simetrie}, \quad (4.5)$$

$$d_{rs} = \frac{d_s}{M_{real}}, \quad (4.6)$$

where $M_{simetrie}$ is the torque given by the symmetric curve and M_{real} is the torque given by the real curve.

The symmetric curves for constructive solutions 5 and 6 and the deviations d_s , d_{rs} from the symmetric curve are presented. The absolute deviation-angle curve for the constructive solutions 5 and 6 is highlighted. In both cases, the deviation is maximum at the extreme of the curve ($\pm 45^\circ$) and minimum at the center of it (0°).

4.1.2.4. Al spacers - Deviation of the torque-angle curve from the ideal curve

The simple linear regression and the ideal curve for the constructive solutions 5 and 6 with Al spacers are presented. In both cases, high torque values are obtained but the torque-angle curve deviates from linearity. The deviations d și d_r from the ideal curve are also presented. The relative deviations values are higher in the case of Al spacers for both constructive solutions. The torque-angle curve falls in the range $[35 \div 45]^\circ$ due to saturation (maximum deviation values). The absolute-angle deviation curve is also represented. In both cases (constructive solutions 5 and 6) the maximum deviation is at 45° .

4.1.2.5. Al spacers - Deviation of the torque-angle curve from the symmetric curve

The symmetric curves for solutions 5 and 6, the deviations d_s , d_{rs} from the symmetric curve and the absolute deviation-angle curve are presented. Deviations from the symmetrical curve have maximum values at the edges of the operating range of the motor and decrease for angles to 0° .

Resizing the auxiliary magnets results in an increase in magnetic flux density with a decrease in the angle between the spacers. In the case of Ol spacers, the torque-angle curve approaches the ideal one for the angular operating range $(-45 \div +45 \text{ grade})$. For Al spacers, a higher maximum torque results but the torque-angle curve deviates from linearity.

4.1.2.6. Study on the numerical analysis of the two-dimensional model for the DC-LATM-CI-C motor

The torque-angle curves are analyzed for the first (initial) model, the model in which an adaptive mesh was used, the model with adaptive mesh in which a filling factor was considered, $k_u = 0.95$ and the experimental model, Fig. 4.6.

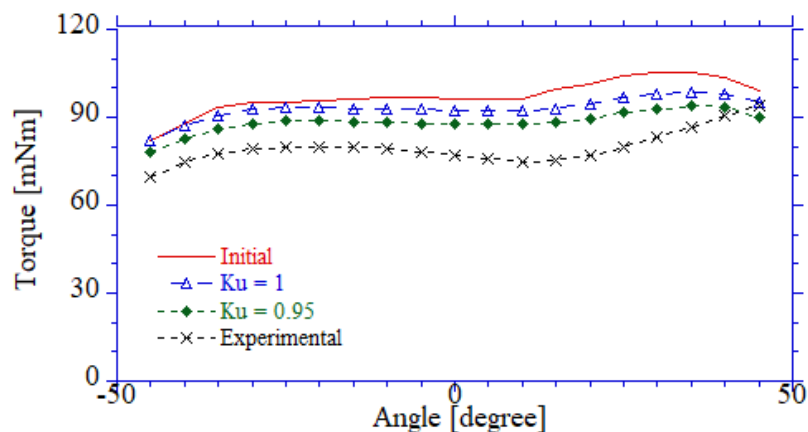


Fig. 4.6. Torque-angle for 2D numerical and experimental models.

Figure 4.6 shows the study of the FEM mesh. The conclusions of the analysis may lead to a decrease in the deviation of the torque-angle curve for the 2D model compared to the torque-angle curve for the experimental model.

The following sub-chapter presents a 3D model of this motor.

4.2. The three-dimensional model

Figure 4.7, a and b show the constructive parts of the model and the FEM mesh used in the numerical analysis. The materials presented in the numerical analysis of the 2D model are used also for the three-dimensional one.

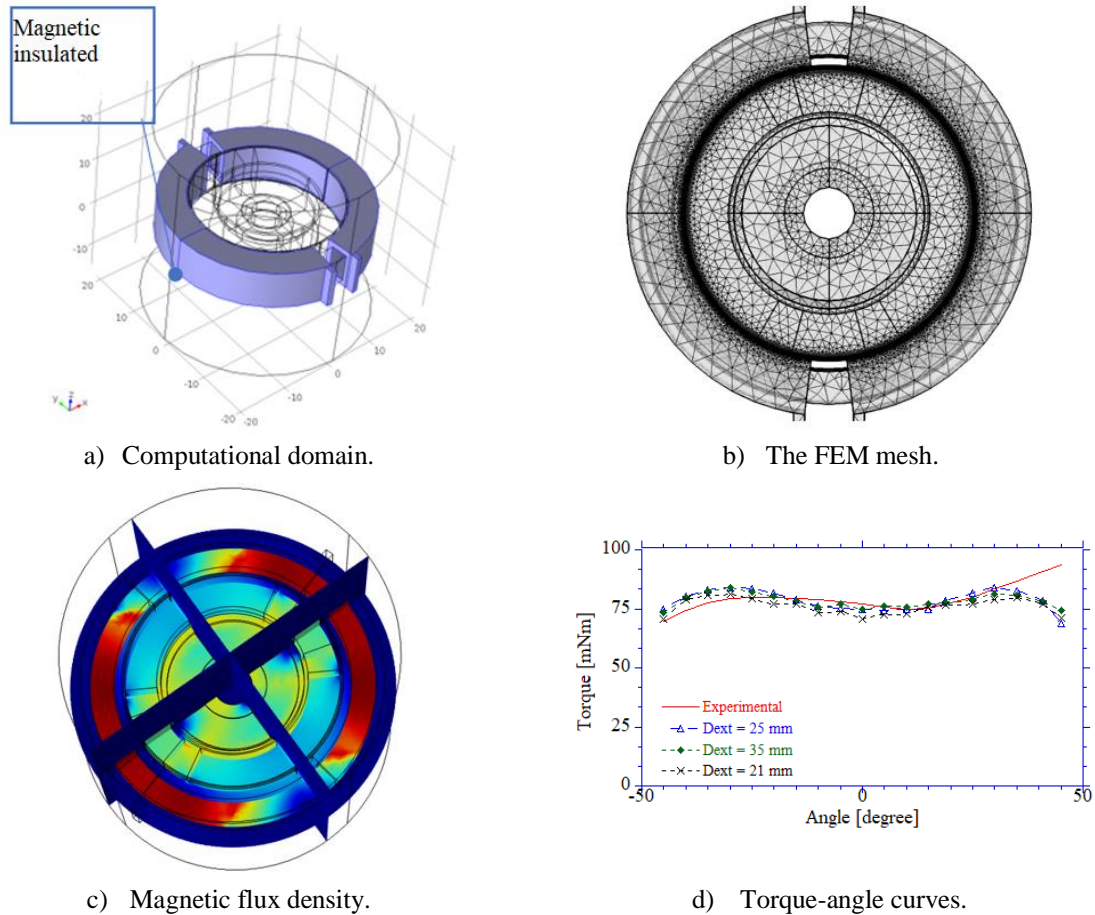


Fig. 4.7. a) Computational domain; b) The FEM mesh; c) Magnetic flux density, max. 2.36 T, min. 0 T; d) Torque-angle curves obtained from 2D and 3D models.

Figure 4.7, c shows the color map of the magnetic flux density. Since the results are strongly influenced by the FEM mesh, accuracy tests were performed, Fig. 4.4, d. The torque-angle curves on the operating range of the motor are represented for the 3D model. In the range $-45^\circ \div 35^\circ$, the calculated torque values are very close to the measured ones. In the range of $40^\circ \div 45^\circ$, the torque decreases and the curve "falls".

4.2.1. Using finite elements of "infinite" type

A study was performed in which the magnetic field problem is closed at a finite distance using finite elements of "infinite" type, Fig. 4.8 a. The used FEM mesh is shown in Fig. 4.8 b.

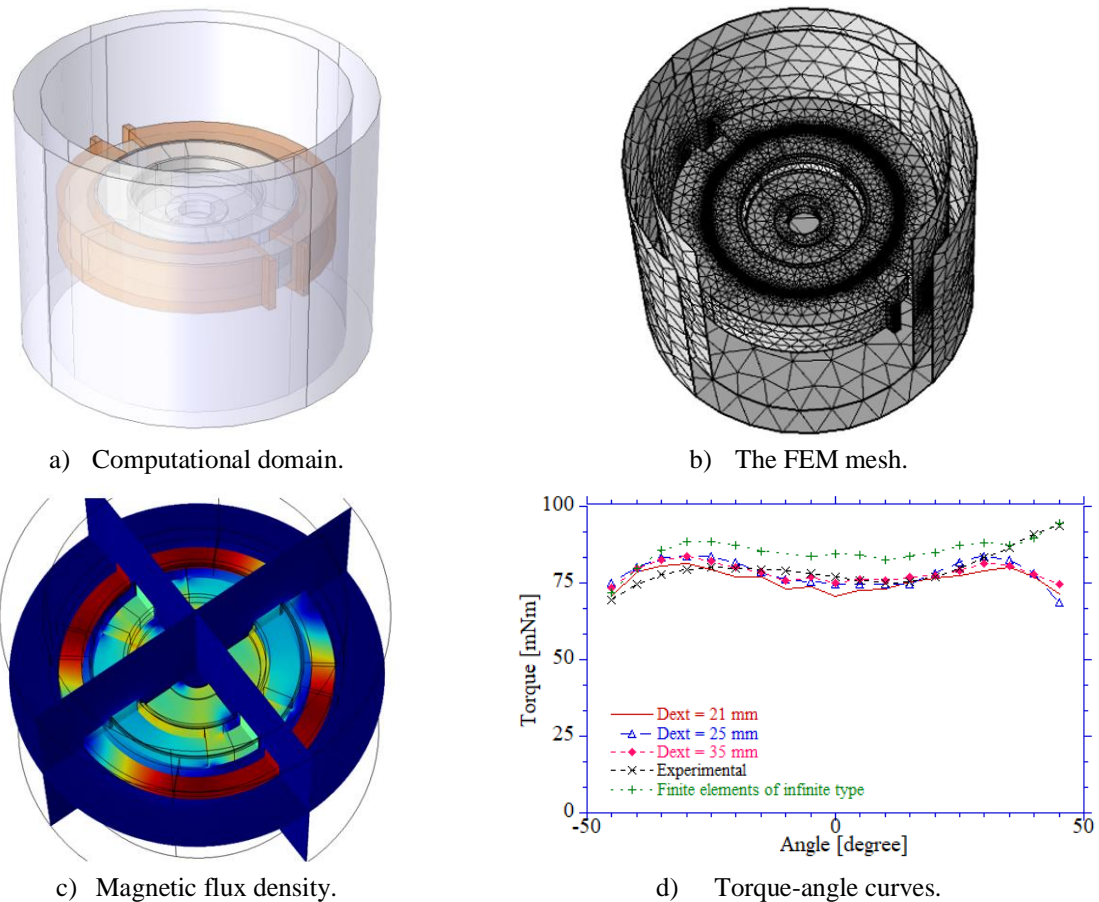


Fig. 4.8. a) Computational domain for DC-LATM-CI-C; b) The FEM mesh; c) Magnetic flux density; d) Torque-angle curves.

Figures 4.8. c and d show the magnetic flux density, respectively the torque curve as a function of angle. The torque values for the 3D model are close to the measured ones.

The selection of DC-LATM is mainly done considering two criteria: uniformity of the torque-angle curve on the operating range and the value of torque required by the beneficiary (nominal value), in a range of $\pm 10\%$. The ideal torque, 74.8 mN m, is considered as a reference. A comparison will be made between the torques measured and calculated in the numerical analysis, 3D model.

The curves on the operating range of the motor for the 3D, 3D model with finite elements of "infinite" type and experimental model are presented. For each model are calculated the simple linear regression, the ideal curve and the absolute and relative deviations from it (d, respectively d_r). In all three cases, high torque values are obtained and the curve deviates from linearity. The values of the relative deviations are higher in the case of the 3D model with finite elements of "infinite" type compared to the other cases. Given the ideal curve that is constant over the operating range, the value of the calculated and measured torques deviates from the value of the ideal torque. From Fig. 4.8. d, it appears that, in the range of $40^\circ \div 45^\circ$, the calculated torque values for the 3D model decrease and the curve "falls" due to saturation. The torque-angle curve for 3D models with finite elements of infinite type presents values of torque close to the values of the ideal curve except the range $40^\circ \div 45^\circ$, where the high value of the relative deviation is given by the high value of the torque (94.6 mNm). Also, the experimental

model shows relative deviations from the ideal curve given by the non-uniformity of the torque-angle curve on the operating range.

The absolute deviation-angle curves for the three models are highlighted and the absolute deviation was calculated. It is found that all models (numerical and experimental) have absolute deviations from the ideal model.

CHAPTER 5 THERMAL MODELING OF A DC LIMITED ANGLE TORQUE MOTOR, DC-LATM-CI-C TYPE

5.1. Introduction

In this chapter, the numerical analysis for heat transfer in DC-LATM-CI-C is presented. This type of motor is built in insulation class F.

3D numerical models are used for the stationary and transient thermal analysis of the presented motor.

Various constructive variants of this type of motor are analyzed to meet its requirements stated in the *technical specification*.

5.2. DC-LATM-CI-C mounted in a non-magnetic stainless-steel device – Variant 1

DC-LATM-CI-C was considered fixed in a device, Fig. 5.1 a. The FEM mesh is shown in Fig. 5.1, b. The heat transfer is carried out by conduction between the motor and the device in which it is mounted and cooling by natural convection to the outer surface. In all cases the numerical study for DC-LATM-CI-C fixed in the device $h = 10 \text{ Wm}^{-2}\text{K}^{-1}$.

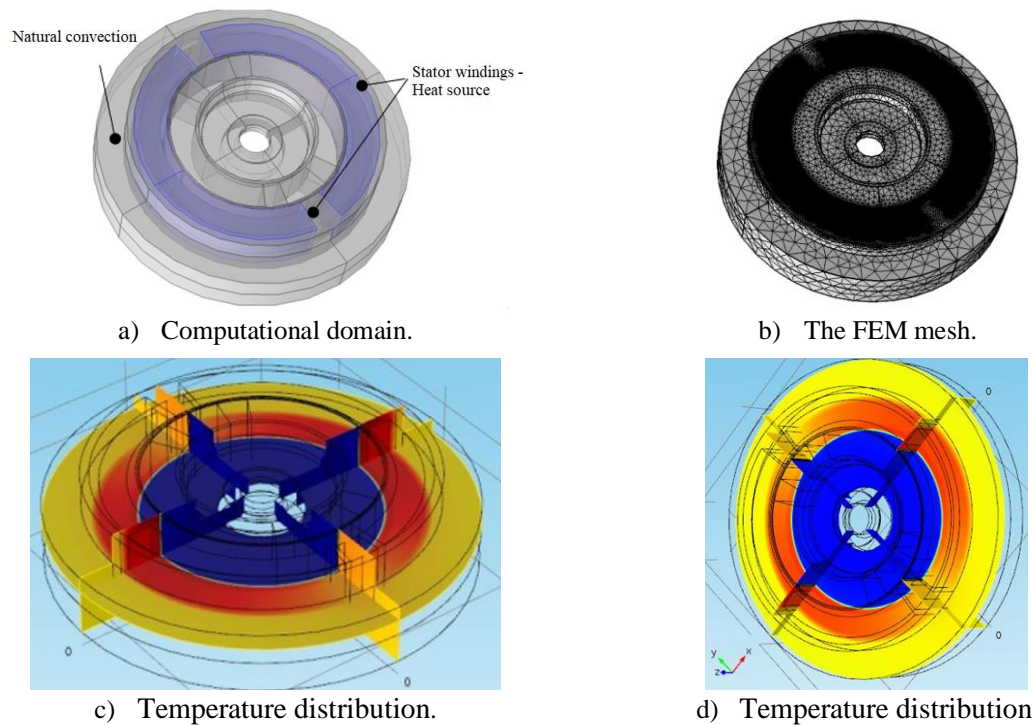


Fig. 5.1. a) Computational domain; b) The FEM mesh; c) Temperature distribution. $T_{\max} = 149 \text{ }^{\circ}\text{C}$ (red), $T_{\min} = 126 \text{ }^{\circ}\text{C}$ (blue); d) Temperature distribution at $t = 3000 \text{ s}$. $T_{\max} = 142 \text{ }^{\circ}\text{C}$ (red), $T_{\min} = 119 \text{ }^{\circ}\text{C}$ (blue).

The results of the numerical study for DC-LATM-CI-C show the distribution of the motor temperature in steady state, Fig. 5.1 c. It is highlighted the evolution in time of the temperature and the time in which the temperature in the windings reaches the maximum allowed temperature, Fig. 5.1, d.

5.3. DC-LATM-CI-C mounted in a non-magnetic stainless-steel device – Variant 2

In the second case that was studied, the motor was considered fixed in an assembly. Its height and width are as large as the motor, Fig. 5.2, a. The FEM mesh used is shown in Fig. 5.2 b. The heat transfer is done by conduction between the motor and the device in which it is mounted and by natural convection to the outer surface. In all cases the numerical study for DC-LATM-CI-C fixed in the device $h = 10 \text{ Wm}^{-2}\text{K}^{-1}$.

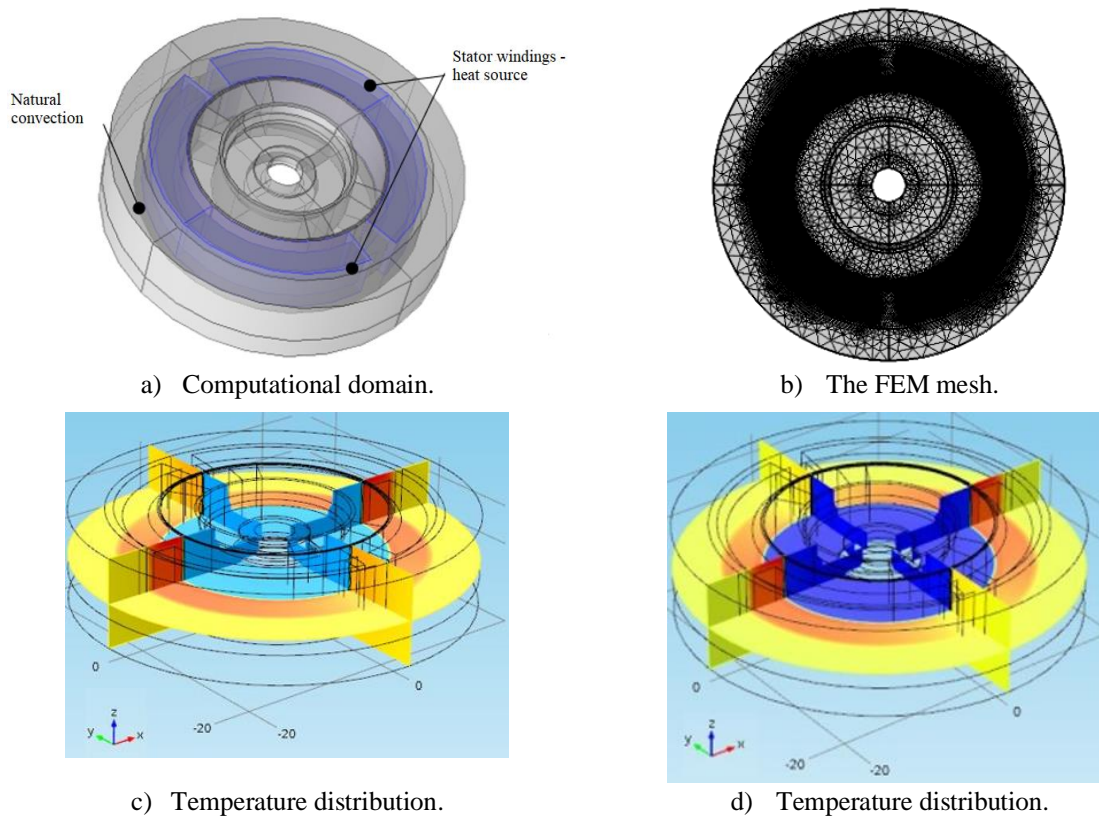


Fig. 5.2. a) Computational domain; b) The FEM mesh; c) Temperature distribution. $T_{\max} = 138 \text{ }^{\circ}\text{C}$ (red), $T_{\min} = 111 \text{ }^{\circ}\text{C}$ (blue); d) Temperature distribution at $t = 3000 \text{ s}$. $T_{\max} = 127 \text{ }^{\circ}\text{C}$ (red), $T_{\min} = 107 \text{ }^{\circ}\text{C}$ (blue).

The results of the numerical study for DC-LATM-CI-C show the distribution of the motor temperature in steady state, Fig. 5.2 c. The evolution in time of the temperature is represented and the time in which the temperature in the windings reaches the maximum allowed temperature, Fig. 5.2 d. The temperature is lower in the second case studied.

5.4. DC-LATM-CI-C mounted in case

Several numerical analyzes were considered by varying the convection heat transfer coefficient, $h = (0 \dots 10) \text{ Wm}^{-2}\text{K}^{-1}$.

Two cases of operation of the studied DC-LATM were highlighted, $I = 1.33 \text{ A}$ and $I = 1 \text{ A}$.

5.4.1. DC-LATM current: $I = 1.33 \text{ A}$

The motor is inserted in a housing, Fig. 5.3 a. The heat transfer is done by conduction between

the motor and the device in which it is mounted and by natural convection to the outer surface.

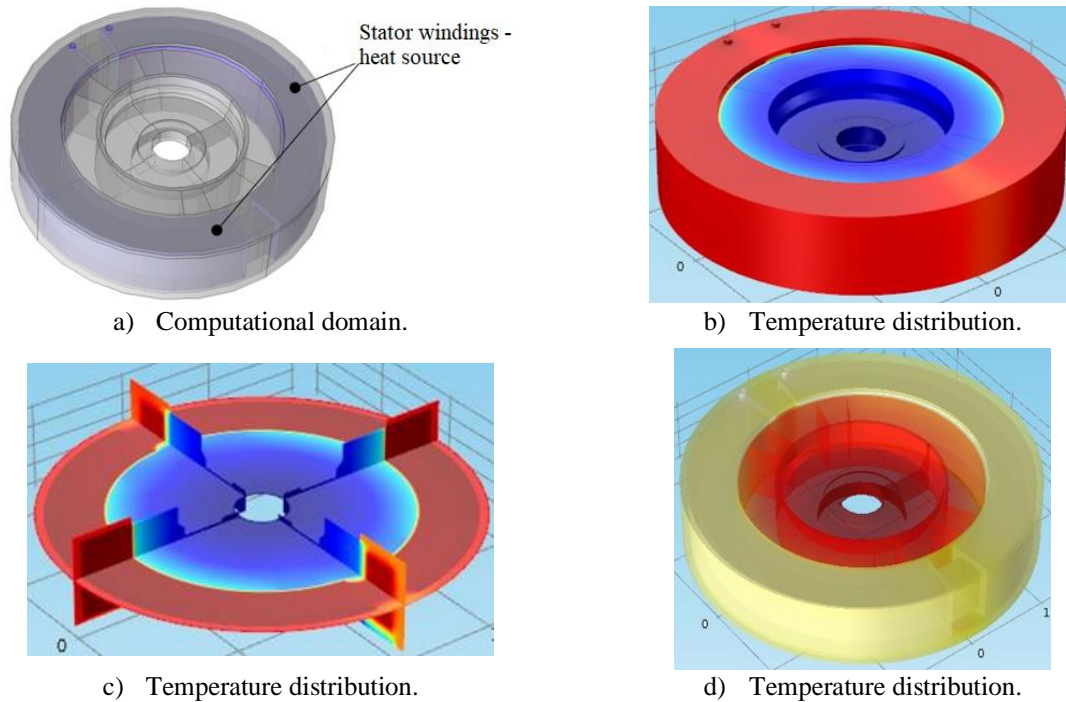


Fig. 5.3. a) Computational domain; b) Fully insulated. $t = 8$ min. $T_{\max} = 178$ °C (red), $T_{\min} = 169$ °C (blue);
 c) $h = 5 \text{ Wm}^{-2}\text{K}^{-1}$. $t = 8$ min. $T_{\max} = 154$ °C (red), $T_{\min} = 145$ °C (blue);
 d) $h = 10 \text{ Wm}^{-2}\text{K}^{-1}$. $t = 8$ min. $T_{\max} = 137$ °C (yellow), $T_{\min} = 127$ °C (red).

The results of the numerical study, Fig. 5.3, b - d, shows the temperature distribution in the motor in transient mode, completely insulated, $h = 5 \text{ Wm}^{-2}\text{K}^{-1}$, $h = 10 \text{ Wm}^{-2}\text{K}^{-1}$, at $t = 0, 6$ and 8 min.

5.4.2. DC-LATM current: $I = 1 \text{ A}$

The heat transfer is done by conduction between the motor and the device in which it is mounted and by natural convection to the outer surface. The computational domain is shown in Fig.5.3, a.

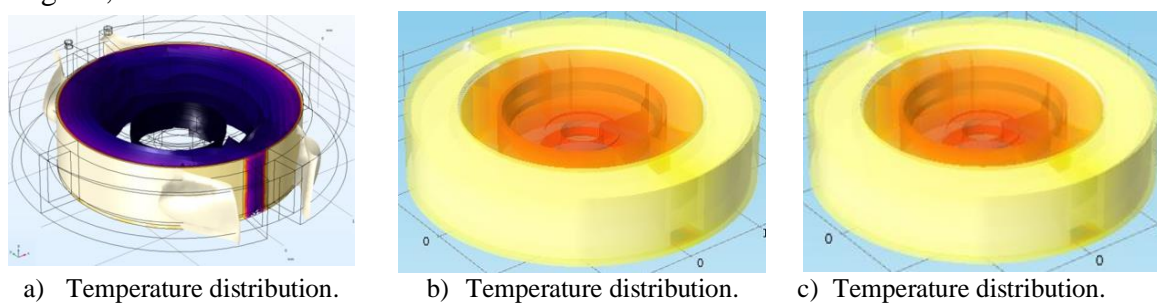


Fig. 5.4. a) Fully insulated. $t = 15$ min. $T_{\max} = 186$ °C (yellow), $T_{\min} = 176$ °C (purple);
 b) $h = 9 \text{ Wm}^{-2}\text{K}^{-1}$. $t = 30$ min. $T_{\max} = 162$ °C (yellow), $T_{\min} = 153$ °C (orange);
 c) $h = 10 \text{ Wm}^{-2}\text{K}^{-1}$. $t = 30$ min. $T_{\max} = 152$ °C (yellow), $T_{\min} = 143$ °C (orange).

The results of the numerical study, Fig. 5.4, a - c, shows the temperature distribution in the motor in transient mode, completely insulated, $h = 9 \text{ Wm}^{-2}\text{K}^{-1}$, $h = 10 \text{ Wm}^{-2}\text{K}^{-1}$, at $t = 15$ and 30 min.

5.5. The experimental results of DC-LATM-CI-C thermal test. Comparison of numerical results with experimental results

The winding temperature of DC-LATM-CI-C was measured at different times, considering two different cases in terms of current.

5.5.1. DC-LATM current: $I = 1 \text{ A}$

Figures 5.5, a and c show the temperatures as a function of time graphs for numerical and experimental results. In Figs. 5.5, b and d are highlighted the maximum temperature as a function of the convection heat transfer coefficient graphs.

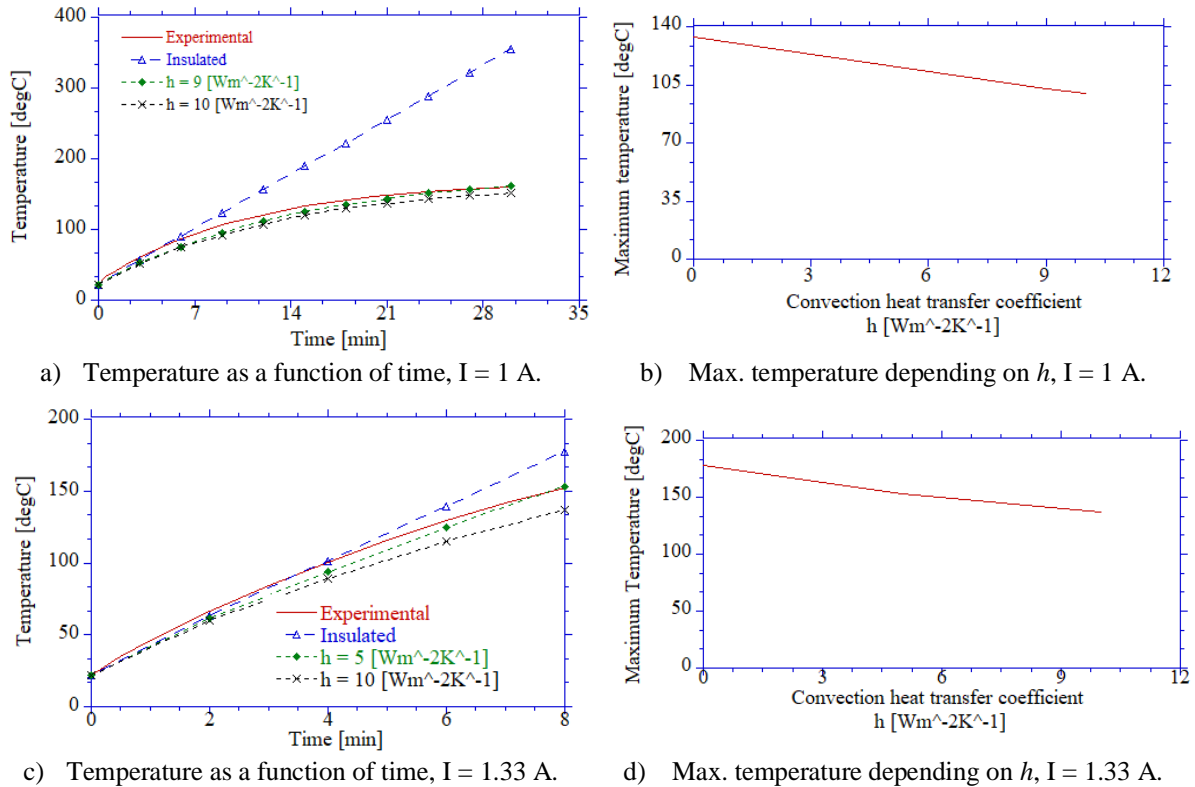


Fig. 5.5. a) and c) Temperature graphics as a function of time for numerical and experimental results; b) and d) Max. temperature graphics depending on h .

If $I = 1 \text{ A}$ the numerical model with $h = 9 \text{ Wm}^{-2}\text{K}^{-1}$ produces the temperature closest to the experimental model. The maximum temperature decreases with increasing convection heat transfer coefficient.

5.5.2. DC-LATM current: $I = 1.33 \text{ A}$

If $I = 1.33 \text{ A}$, the numerical model with $h = 5 \text{ Wm}^{-2}\text{K}^{-1}$ has the temperature values as a function of time closest to the experimental model (Fig. 5.5, d).

CHAPTER 6. STUDY ON THE DC-LATM APPROACH IN VARIOUS FIELD APPLICATIONS - MATERIALS AND TECHNOLOGICAL FLOW

A study on DC-LATM for military and aerospace applications is presented. The results of this analysis are inputs to the approach of this type of motor for space applications. The

technological flow of DC-LATM is presented. This is the next step after establishing the numerical solution and the first stage in the manufacturing process. Then adapt the manufacturing steps for the space area according to the environmental requirements of the motor application.

The motor is manufactured on components, as highlighted in the DC-LATM flow chart. The first step is the analysis of the selection criteria of the materials used. This depends on the level of maturity of the product and the constraints of the space domain.

6.1. Specifications or standards

The selection criteria of materials and processes are presented: standards, procedures corresponding to space applications etc. and documents on materials and processes.

6.2. Selection of non-suitable materials for space applications

For materials about which there is no information, developers must justify the proposed selection and use to obtain approval.

6.2.1. Purchase of materials

Databases that combine data on materials from several sources are presented. It clarifies how to complete the lists of materials and processes as well as the applicable factors. It is explained and presented diagrams on the choice of materials (considering their sensitivity from the point of view of the working environment) and the essential processes used in the manufacture of the motor, including the request for approval document for their use.

For the space domain, the manufacturing and assembly sequence is documented in a manufacturing flow. Upon completion of the steps in the diagrams presented, the critical processes and implicitly the motor components will be qualified.

To fulfill the traceability condition, the doctoral thesis presents the components of a DC-LATM within the technological flow. At the end of it is obtained DC-LATM, Fig. 6.1.

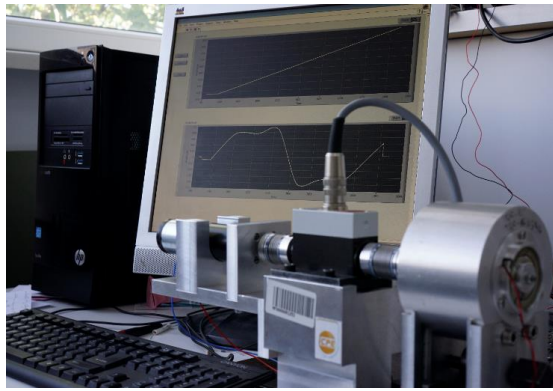


Fig. 6.1. DC-LATM-CI-C at the final of technological process.

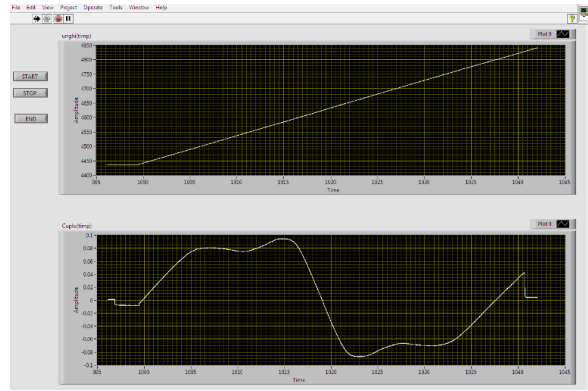
CHAPTER 7. DC LIMITED ANGLE TORQUE MOTOR – EXPERIMENTALS MODELS

The experimental model is subjected to a set of DC-LATM measurements and tests [4, 28] (obtaining the torque-angle curve on the operating range).

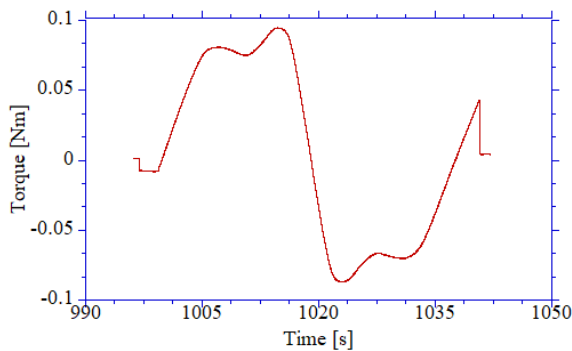
The measuring stand for DC-LATM, the data measured by the transducer and the obtained results are presented, Fig. 7.1, a - c.



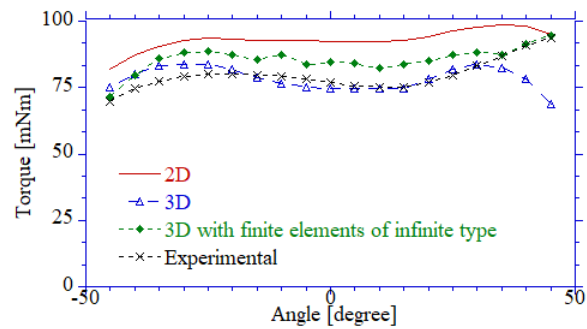
a) Measurement stand.



b) Measured data by transducer.



c) Torque-time curve.



d) Torque-angle curves.

Fig. 7.1. a) Measurement stand for DC-LATM at the time of data acquisition; b) Measured data by transducer; c) Torque-time curve for DC-LATM-CI – C; d) Torque-angle curves comparison for numerical and experimental models.

The maximum value of the torque is about 94 mN m. The curve is not constant and has a certain asymmetry with respect to the torque axis.

The torque values in the 2D approximation are higher than the experimental model. Fig. 7.1, d. This aspect also emerges from the values of the relative error presented in the doctoral thesis.

Using the same measuring stand, the characteristics of another DC-LATM from the same motor family were checked. Torque and angle measurements were performed for DC-LATM-CI-D using the same torque transducer with angle transducer. For the rated motor current, $I = 2.2$ A, a maximum torque equal to 44 mN m is obtained. This value is in accordance with the technical requirement of DC-LATM. Experimental values may deviate from the nominal value [4] within $\pm 10\%$.

CONCLUSIONS

C.1. General conclusions

The scientific research aimed to study DC-LATM, which presents a topic of interest due to its construction and applications.

The approach in the analysis of a DC-LATM motor was presented (from the point of view of a well-formulated problem, of the physical model, of the mathematical and numerical modeling).

For the calculation of specific DC-LATM sizes and characteristics, different configurations for three types of DC-LATM were studied, using numerical modeling.

The two- and three-dimensional models developed and presented allowed the evaluation of the sizes and characteristics for each DC-LATM.

Only one type of DC-LATM was chosen and various studies were performed on the use of finite elements of "infinite" type.

The influence of the rotor constructive solutions on the torque-angle curve was studied.

The selection criteria of DC-LATM were presented and by considering an ideal torque, the measured torque and the calculated torque in the numerical analysis, the 3D model, were compared.

The simple linear regression and the ideal curve for each of the studied models were presented and the absolute deviation, the relative deviation and the absolute deviation-angle curve were calculated.

The development of numerical models for evaluating the thermal behavior of DC-LATM chosen for the study led to a correct characterization of the motor in terms of operation.

The technological flow, the realization of the experimental model for DC-LATM chosen for the study and the comparison of the torque-angle curves for the numerical and experimental models completes the scientific research carried out within the doctoral studies.

C.2. Original contributions

The personal contributions to this paper are the following:

- Improving the value of the main parameter of DC-LATM-CI-B and DC-LATM-CI-C. This was done by studying the influence of the rotor constructive solutions on the torque-angle curve for the two motors. Different constructive solutions of the rotor were analyzed by resizing the auxiliary magnets and by using two types of materials for spacers, OI and AI.
- Calculation of the deviation of the torque-angle curve from the ideal and symmetrical one and the absolute deviation-angle curve for each presented variant - Definition of a new estimator as well as a new interpretation of that statistic.
- Analysis of the thermal behavior of DC-LATM-CI-C.
 - Conceptual model of the devices in which the motor has been integrated.

- Carrying out a thermal experiment in which two different cases were considered in terms of DC-LATM current: $I = 1 \text{ A}$ and $I = 1.3 \text{ A}$. Measuring the temperature at different times (as a function of current) and making the temperature graph ($T_{\text{amb}} = 22 \text{ }^\circ\text{C}$) as a function of time.
- Design of process diagrams for the selection and approval of materials, acceptance of materials, selection and approval of processes and qualification of processes for components.
- Design of the logic diagram of the measuring stand for DC-LATM, acquisition and processing of data measured by the transducer for DC-LATM-CI-C and DC-LATM-CI-D.
 - Performing torque and angle measurements using the torque transducer with angle transducer, for $I = 50\% \cdot I_n \text{ A}$, $I = 50\% \cdot I_n$ and $I = 50\% \cdot I_n \text{ A}$, where $I_n = 2.2 \text{ A}$. Realization of torque and angle graphs as a function of time.

C.3. Development perspectives

From the above conclusions, certain issues require further and new investigations. Through these analyzes, a deep understanding and a complete approach to the study of DC-LATM behavior is obtained. The scientific research carried out and the results obtained represent input for future analyzes. The following directions of further development are considered:

- Completing the study on the behavior of DC-LATM motors in space applications from thermal point of view. Numerical analyzes will be considered in which the heat transfer will be done using radiation and conduction.

The special operating conditions and applications in which DC-LATM are used require numerical studies of the thermal field. Numerical studies are essential in the development stage for defining the behavior of the motor in various operating conditions. In the space field, determining the DC-LATM behavior in the absence of any cooling source is essential. Numerical analyzes will be considered in which the heat transfer will be performed only by conduction and radiation.

- Numerical study of thermal and mechanical stresses for DC-LATM.

In the operation of special electric machines, thermal and mechanical stresses are extremely important. Therefore, numerical studies for these motors are intended to be performed to ensure their proper operation in environments with difficult conditions and high reliability.

- Study of a motor chosen for a space application. It involves design, analysis of motor behavior in space conditions and its path from prototype to qualified model.

ANNEX A1 – GENERAL FORM FOR THE MAGNETIC FIELD

In Chapter 2, subchapter 2.2, section 2.2.1, was presented the reduced form for the magnetic field, applicable in the studied problem, the DC-LATM study.

In this appendix, the study and the general form of the magnetic field, the law of the magnetic circuit, the law of the magnetic flux and the general theorems of the electromagnetic field are

presented.

ANNEX A2. TRL LEVELS

The technological maturity levels.

ANNEX A3. ESA STANDARDS - SELECTION

The ESA standards according to which materials and processes are chosen.

ANNEX A4. MATERIALS LIST SPACEMATDB - SPACE MATERIALS DATABASE

The list of materials from the SPACEMATDB database.

ANNEX A5. MATERIALS USED IN SPACE APPLICATIONS AND THE RELEVANCE OF SPACE PARAMETERS ON MATERIAL SELECTION

The materials used in space applications and the relevance of space domain constraints on material selection.

ANNEX A6. MATERIALS LIST - DML

Aspects related to the list of materials (environmental code, size and status of approval) are highlighted.

ANNEX A7. PROCESSES LIST - DPL

The status approval of the processes list.

ANNEX A8. THE STAGES OF THE TECHNOLOGICAL PROCESS OF A DC-LATM

The stages of the technological process for a DC-LATM.

BIBLIOGRAPHY

- [1] R. Măgureanu, Mașini electrice speciale pentru sisteme automate, Editura Tehnică, București, 1981.
- [2] Moog Catalogue, Direct Drive Brushless DC Torque Motors, 2013.
- [3] Precilec Catalogue, Permanent magnet generators and motors, 2013.
- [4] Icpe Catalogue, Special Electric Machines, 2019.
- [5] BENTAL Motion Systems, "Brushless Motors", 2013.
- [6] R. Obreja, I.R. Edu, "Limited Angle Torque Motors having high torque density, used in accurate Drive Systems", in Acta Polytechnica, **Vol. 51**, Nr. 5, 2011, pp.75-83.
- [7] M.I. Andrei, N.M. Modreanu, Modelarea numerică a unui motor de cuplu cu unghi limitat cu două canale, [Numeric Modelling of a Two-Channel Limited Angle Torque Motor], in EEA – Electrotehnică, Electronică, Automatică, Editura. ELECTRA, **Vol. 62**, Nr. 1, 2014, pp. 26-31.
- [8] C. I. Mocanu, Teoria câmpului electromagnetic, Editura Didactică și Pedagogică, București, 1984.
- [9] www.motioncontroltips.com
- [10] A. M. Morega, Surse de energie. Note de curs, Facultatea de Electrotehnică, Universitatea POLITEHNICA din București, 2018 - 2019.
- [11] A.M. Morega, J.C. Ordonez, J.V.C. Vargas, S. Kosaraju, "A Finite Element Method Analysis and Optimization of a Polymer Electrolyte Membrane Fuel Cell with Interdigitated Flow Field Design", International Journal of Energy Technologies and Policy (IJETP), Special Issue: Computational Fluid Dynamics Simulations in Energy Technologies and Processes.
- [12] Icpe, Componente electromecanice pentru sisteme high-tech direct drive realizate cu linii tehnologice flexibile – HTDD, etapa I, Oct. 2013, <http://www.icpe.ro/htdd/ro>.
- [13] Icpe, Componente electromecanice pentru sisteme high-tech direct drive realizate cu linii tehnologice flexibile – HTDD, etapa II, Oct. 2013, <http://www.icpe.ro/htdd/ro>.
- [14] A. Popescu, Elemente Fundamentale de transfer de căldură, Editura Eurobit, Timișoara, 2003.
- [15] O.C. Zienkiewicz, The Finite Element Method. McGraw-Hill, 1977.
- [16] M. Blumenfeld, Introducere în metoda elementelor finite, Ed. Tehnică, 1995.
- [17] D. Gârbea, Analiză cu elemente finite, Ed. Tehnică, 1990.
- [18] Ș. Maksay, D. Bistriian, Introducere în metoda elementelor finite, ISBN 978-973-667-324-5, Iași, 2007.
- [19] M. Modreanu, A. Morega, "Analiza numerică a fenomenelor electromagnetice și termice într-un motor de curent continuu de mică putere", [Numerical Analysis of the Electromagnetic and Thermal Phenomena in a DC Motor of Low Power], în Sesiunea omagială de comunicări științifice "55 de ani de activitate a Grupului ICPE în dezvoltarea sectorului electrotehnic", București, 20–21 Sept. 2005.
- [20] M. Modreanu, M. Morega, "Evaluarea numerică și experimentală a unui motor de curent continuu cu magneți permanenți [Numerical and Experimental Evaluation of a DC Motor with Permanent Magnets]", in Simpozionul Actualități și Perspective în domeniul mașinilor electrice, Ediția a V-a, Universitatea POLITEHNICA din București, Catedra de Mașini, Acționări și Materiale, ISSN 1843-5912, 13–14 oct. 2009.
- [21] T. Tudorache, M. Morega, "Calculul 3D al încălzirii unui motor de c.c. de mică putere folosind metoda elementului finit [The 3D Calculation of Heating a DC Motor Low Power using the Finite Element Method]", in Simpozionul Actualități și Perspective în domeniul mașinilor electrice, Ediția a V-a, Universitatea POLITEHNICA din București, Catedra de Mașini, Acționări și Materiale, ISSN 1843-5912, 13–14 oct. 2009.
- [22] O. Craiu, A. Machedon, "3D Finite Element Thermal Analysis of a Small Power PM DC Motor–Optim", in 12th International Conference on Optimization of Electric and Electronic Equipment, Brasov, 20-22 mai 2010.
- [23] O. Craiu, A. Machedon, "Modele electromagnetice și termice pentru servomotoare de c.c. cu magneți permanenți [Electromagnetic and Thermal Models for DC Servomotors with Permanent Magnets]", in Tendințe de dezvoltare în fabricația mașinilor electrice și cerințe actuale ale UE, Universitatea POLITEHNICA din București, 15 Apr. 2010.
- [24] O. Craiu, M. Modreanu, "Studiu experimental și numeric al încălzirii unui motor de c.c. de mică putere, în condiții variate de funcționare [Experimental and Numerical Study of Heating of a DC Motor of Low Power, under Varied Operating Conditions]", Simpozionul de mașini electrice SME 2010, București, 7 –

8.10.2010.

- [25] *J.-M. Jin*, "The Finite Element Method in Electromagnetics", in John Wiley and Sons Publisher, New York, 2002.
- [26] *I. Ionică, M. Modreanu, A. Morega*, "Numerical Studies on a DC, Limited Angle, Torque Motor" in SIELMEN 2015 – Proceedings of the 10th International Conference on Electromechanical and Power Systems, Editura. ALMA, Chişinău, 8-9 Oct. 2015, pp 249-255.
- [27] Comsol Multiphysics, www.comsol.com.
- [28] *M.I. Andrei, N.M. Modreanu, M. Guţu, L. Ghiţulescu*, "Sistem de măsură asistat de calculator pentru caracterizarea motoarelor de cuplu cu unghi limitat" [Computer Aided Measurement System for the Characterization of Limited Angle Torque Motors], in EEA - Electrotehnică, Electronică, Automatică, Editura. ELECTRA, Vol. 62, Nr. 3, ISSN 1582-5175, Iun-Sept 2014.
- [29] *M. Morega*, Maşini şi acţionări electrice. Note de curs, Facultatea de Electrotehnică, Universitatea POLITEHNICA din Bucureşti, 2007.
- [30] *D. Stoia*, Excited DC motors with permanent magnets, Editura Tehnică, Bucureşti 1983.
- [31] *P.R. Upadhyay, K.R. Rajagopal, B.P. Singh*, "Computer aided design of an axial-field permanent magnet brushless dc motor for an electric vehicle", in Journal of Applied Physics, Vol. 93, nr.10, Mai 2003, pp.8689-8691.
- [32] *P.R. Upadhyay, K.R. Rajagopal*, "FE Analysis and Computer-Aided Design of a Sandwiched Axial-Flux Permanent Magnet Brushless DC Motor," in IEEE Transactions on Magnetics, Vol. 42, nr.10, Oct. 2006, pp.3401-3403.
- [33] *P.R. Upadhyay, K.R. Rajagopal*, "FE analysis and CAD of radial-flux surface mounted permanent magnet brushless DC motors", in Digests of the IEEE International Magnetics Conference -INTERMAG Asia 2005, 4–8 Aprilie 2005, pp.729-730.
- [34] *R. Obreja, I.R. Edu*, "Limited Angle Torque Motors having high torque density, used in accurate Drive Systems", in Acta Polytechnica, Vol. 51, Nr. 5, 2011, pp.75-83.
- [35] *C. Ghiţă*, Elemente fundamentale de maşini electrice, Editura PRINTECH, Bucureşti, 2002.
- [36] *M.I. Andrei, M. Modreanu, L. Ghiţulescu*, "ACES Methodology for a DC Limited Angle Torque Motor", in Revue roumaine des sciences techniques, Série Électrotechnique et Énergétique.
- [37] *D. Meeker*, User's Manual for Finite Element Method Magnetics – FEMM, ver. 4.2, Oct. 2010.
- [38] *N. Vasile*, Ingineria Electrică – Probleme actuale, Editura Electra, Bucureşti, 2010.
- [39] *A. Hemeida, P. Sergeant*, "Analytical modeling of surface PMSM using a combined solution of Maxwell's equations and magnetic equivalent circuit", IEEE Transactions on Magnetics, Vol. 50, 12, art. 7027913, 2014.
- [40] *A. Boglietti, A. Cavagnino, D.A. Staton*, "Thermal Analysis of TEFC Induction Motors", Proc. of IEEE International Conference PEDS 2003, Singapore, 2003.
- [41] *A. Boglietti, A. Cavagnino, M. Lazzari, M. Pastorelli*, "A simplified thermal model for variable-speed self-cooled industrial induction motor", IEEE Transactions on Industry Application, Vol. 39, Issue 4, 2003, pp. 945 – 952.
- [42] *A. Cassat, C. Espanet, N. Wavre*, "BLDC motor stator and rotor iron losses and thermal behavior based on lumped schemes and 3-D FEM analysis", IEEE Transactions on Industry Application, Vol. 39, Issue 5, 2003, pp. 1314 – 1322.
- [43] *E. Lebenhaft*, "Field Evaluation of Slip-Dependent Thermal Model for Motors with High-Inertia Starting", Petroleum and Chemical Industry Technical Conference, 2007. PCIC '07, pp. 1 – 5, 2007.
- [44] *H.P. Liu, V. Lelos, C.S. Hearn*, "Transient 3-D thermal analysis for an air-cooled induction motor", Proc. of IEEE International Conference IEMDC 2005, 2005, pp. 417 – 420.
- [45] *R. Bernard, R. Glises, D. Chamagne*, "3D thermal study of a low power electric motor with Flux3D", Flux-Magazine, No. 37, 2001, pp. 10 – 11.
- [46] *T. F. Pirious, A. Razek*, "Finite element analysis in electromagnetic systems accounting for electric circuits," IEEE Trans on Magnetics, Vol.29, No.2, March 1993, pp.1669-1675.
- [47] *P. B. Zhou*, "Numerical analysis of electromagnetic fields," Springer-Verlag, 1993.
- [48] *M. C. Leu, R. A. Aubrecht*, "Feasible and Optimal, Designs of Variable Air gap Torque Motors" Journal

- of Engineering for Industry, ASME, 1991.
- [49] A. G. Mikerov, "Brushless DC torque motors quality level indexes for servo drive applications", EUROCON'09 IEEE, 2009.
- [50] Y. Zhang, "High Performance DSP based Servo Drive, Control for a Limited Angle Torque Motor" Thesis at Loughsborough University, England, 1997.
- [51] Z. Jibin, Y. Guodong, X. Yongxiang, C. Xia, L. Yong, and W. Qian, Development of a Slotless Limited-Angle Torque Motor for Reaction Wheels Torque Measurement System, IEEE TRANSACTIONS ON MAGNETICS, **Vol.** 50, No. 11, November 2014.
- [52] N. Z. Reza, M. Mojtaba and A. Cavagnino, Analysis, Optimization, and Prototyping of a Brushless DC Limited-Angle Torque-Motor with Segmented Rotor Pole Tip Structure, IEEE TRANSACTIONS ON INDUSTRIAL ELECTRONICS, **Vol.** 62, No. 8, August 2015.
- [53] H. I. Lee and M. D. Noh, "Optimal design of radial-flux toroidally wound brushless dc machines," IEEE Trans. Ind. Electron., **Vol.** 58, no. 2, Feb. 2011, pp. 444–449.
- [54] M. F. Hsieh and Y. C. Hsu, "A generalized magnetic circuit modeling approach for design of surface permanent-magnet machines," IEEE Trans. Ind. Electron., **Vol.** 59, no. 2, Feb. 2012, pp. 779–792.
- [55] C. C. Tsai, S. C. Lin, H. S. Huang, and Y. M. Cheng, "Design and control of a brushless dc limited-angle torque motor with its application to fuel control of small-scale gas turbine engines," Mechatronics, **Vol.** 19, no. 1, Feb. 2009, pp. 29–41.
- [56] R. Nasirizarandi, H. M. Kelk, F. Toorani, and H. Farahmandzad, "Comprehensive design of a toroidally-wound limited angle torque motor," Int. Rev. Elect. Eng., **Vol.** 6, no. 1, Feb. 2011, pp. 198–206.
- [57] C. Dawson and H. R. Bolton, "Performance prediction of a wide-angle limited-motion rotary actuator," Proc. Inst. Elect. Eng., **Vol.** 125, no. 9, Sep. 1978, pp. 895–898.
- [58] P. M. Krishna and N. Kannan, "Brushless dc limited angle torque motor," in Proc. IEEE Int. Conf. Power Electron., Drives Energy Syst. Ind. Growth, New Delhi, India, 1996, pp. 511–516.
- [59] G. Bramerdorfer, S. M. Winkler, M. Kommenda, G. Weidenholzer, S. Silber, G. Kronberger, M. Affenzeller, W. Amrhein, "Using FE calculations and data-based system identification techniques to model the nonlinear behavior of PMSMs," IEEE Trans. Ind. Electron., **Vol.** 61, no. 11, Nov. 2014, pp. 6454–6462.
- [60] P. Hekmati and M. Mirsalim, "Design and analysis of a novel axial flux slotless limited-angle torque motor with trapezoidal cross section for the stator," IEEE Trans. Energy Convers., **Vol.** 28, no. 4, Dec. 2013, pp. 815–822.
- [61] C. Dawson and H. R. Bolton, "Design of a class of wide-angle limited-rotation rotary actuators," Proc. Inst. Elect. Eng., **Vol.** 126, no. 4, Apr. 1979, pp. 345–350.
- [62] Y. Zhang, I.R. Smith, J.G. Kettleborough, "Performance evaluation for a limited-angle torque motor," IEEE/ASME Trans. Mechatronics, **Vol.** 4, no. 3, Sep. 1999, pp. 335–339.
- [63] C. R. Tufts, "Selecting the correct magnetic material," in Proc. IEEEEIC/ ICWA, Chicago, IL, USA, 1995, pp. 65–68.
- [64] G. P. Widdowson et al., "Computer-aided optimization of rare-earth permanent magnet actuators," in Proc. IET Int. Conf. Comput. Electromagn., London, U.K., 1991, pp. 93–96.
- [65] M. Roohnavazfar, M. Houshmand, R. Nasirizarandi, and M. Mirsalim, "Optimization of design parameters of a limited angle torque motor using analytical hierarchy process and axiomatic design theory," Prod. Manuf. Res., **Vol.** 2, no. 1, May 2014, pp. 400–414.
- [66] J. Pyrhonen, T. Jokinen, and V. Hrabovcová, "Design of rotating electrical machines," in Front Matter. Hoboken, NJ, USA: Wiley, 2008.
- [67] V. N. Mittle and A. Mittal, Design of Electrical Machines. New Delhi, India: N.C. Jain, 2002.
- [68] Li Y. – X., Wang T., Zhang W., Dynamic Performance Analyze of Swing Angle Torque Permanent Magnet Motor under Different Structure and Winding Parameters, Proceeding of the 2015 IEEE International Conference on Information and Automation Lijiang, China, August 2015.
- [69] K. J. Binns, P. J. Lawrenson, and C. W. Trowbridge, The Analytical and Numerical Solution of Electric and Magnetic Fields. Wiley, 1994.
- [70] <https://ecss.nl/>
- [71] <http://www.rosa.ro/index.php/en/>

- [72] **I. Ionică, M. Modreanu, A. Morega, C. Boboc** - Studii numerice pentru mașini electrice speciale de tipul motoarelor de cuplu cu unghi limitat, EEA – Electrotehnică, electronică și automată, revistă indexată în 6 baze de date internaționale, cotaată B+ de CNCIS; vol. 64, nr. 3, Articolul 2, Iulie-Septembrie 2016, Editura ELECTRA, 2016, pp. 12-19, ISSN: 1582-5175.
- [73] **I. Ionică, M. Modreanu, A. Morega, C. Boboc** - Design and Modeling of a Hybrid Stepper Motor, The 10th International Symposium on Advanced Topics in Electrical Engineering, Bucharest, România, March 23-25, 2017, pp.192-195, ISBN: 978-1-5090-5160-1.
- [74] **I. Ionică, M. Modreanu, A. Morega, C. Boboc** - Numerical analysis of a hybrid stepper motor for the electromagnetic torque calculation, The 11th International Symposium on Advanced Topics in Electrical Engineering, Bucharest, România, March 28-30, 2019, pp.1-6, ISBN: 978-1-7281-0101-9/19/\$31.00 ©2019 IEEE.
- [75] **I. Ionică, M. Modreanu, A. Morega, C. Boboc** – DC Limited Angle Torque Electrical Motor, Scientific Bulletin of University „Politehnica” of Bucharest, 2019, series C, Electrical Engineering and Computer Science, No. 1, Vol. 81, Iss. 1, pp.193-202, ISSN 2286-3540.
- [76] **I. Ionică, M. Modreanu, A. Morega, C. Boboc** – Magnetic field models for a dc, torque motor, Buletinul Institutului Politehnic din Iași, Secția Electrotehnică, Energetică și Electronică, 2015, Fasc. 4, Tomul LXI (LXV), Editura Politehnicum, pp. 53-60, ISSN: 1223-8139.
- [77] **I. Ionică, M. Modreanu, A. Morega, C. Boboc** – Studii de câmp electromagnetic și termic pentru mașini electrice speciale, Actualități și perspective în domeniul mașinilor electrice, University POLITEHNICA of Bucharest, Faculty of Electrical Engineering, Department of Electrical Machines, Materials and Drives, București, România, 2019, ISSN / ISSN-L: 1843-5912, <https://www.doi.org/10.36801/apme.2019.1.13>.
- [78] **I. Ionică, M. Modreanu, A. Morega, C. Boboc** – Tridimensional modeling for a dc, limited angle, torque motor of size 16th, International Conference and Exposition on Electrical and Power Engineering, Iași, România, October 20-22, 2016, pp. 235-239, ISBN: 978-1-5090-6129-7/16/\$31.00 ©2016 European Union.
- [79] **I. Ionică, Ș. Tănase, I.-M. Nicola, C.-B. Oprea, A.-C. Covrig, A.-C. Stancu** – Iepe, a Worldwide Brand and Best Romanian Electric Motor Developer and Manufacturer for High-tech Industry and Space, Actualități și perspective în domeniul mașinilor electrice, University POLITEHNICA of Bucharest, Faculty of Electrical Engineering, Department of Electrical Machines, Materials and Drives, București, România, 2019, ISSN / ISSN-L: 1843-5912, <https://www.doi.org/10.36801/apme.2019.1.16>.